Tampereen yliopisto

Nina Olenius

EXAMINING TRIGENERATION WITH HIGH TEMPERATURE HEAT STORAGE

A Techno-Economic Analysis

Master of Science Thesis
Faculty of Engineering and Natural Sciences
Examiners: University Lecturer Henrik Tolvanen &
Principal Lecturer Aki Korpela
June 2022

ABSTRACT

Nina Olenius: Examining trigeneration with high temperature heat storage
Master of Science Thesis
Tampere University
Environmental and Energy Engineering
June 2022

As the world is trying to shift away from fossil fuels in energy production, it has become important to find solutions to the problem of maintaining the stability of the grid as renewable energy sources are not always available. Energy storages offer one solution to this problem and probably the most well-known energy storages are batteries. The issue with batteries, though, is their price, which is very high especially with larger batteries. An option for batteries could be a heat storage, where the energy is stored in form of heat.

Energy storages bring a totally different way of managing one's energy demands to the table. They allow for more independent energy supply and a possibility for off-grid applications. An energy storage can usually match the energy demand of only one form of energy unless it is combined with other systems e.g., heating resistor.

The aim of this thesis was to study trigeneration, its applications and compare two different systems that have trigeneration production. The systems that were studied in this thesis are a heat storage system utilizing organic Rankine cycle and absorption chiller and a lithium-ion battery system utilizing a heat pump. Trigeneration is a means of energy production, where electricity, heating, and cooling are produced simultaneously. With the heat storage system, electricity is produced in the organic Rankine cycle and heating and cooling are produced with the absorption chiller. In the lithium-ion battery system, electricity is discharged from the battery and heating and cooling are produced with the heat pump.

The technologies in both systems were studied and an Excel simulation program was constructed for both systems to study their performance in certain conditions. An economic feasibility analysis was also performed on both systems. The simulation was run for three different cases: a normal sunny day, a cloudy day, and a day with no solar energy available. The application chosen for this study was a hospital. Other possible applications could have been, for example, a hotel, an office building, or a university. The results showed that both systems performed as well in the simulation. They could match the energy need of the hospital in the first two cases but in the third case with no solar energy available, each energy storage was empty before noon. A bigger difference in comparing these systems was found in the economic feasibility analysis. The investment costs of the main components in these systems were divided between their life span using the annuity method. The results of this analysis show, that the lithium-ion battery is the most expensive component of all the components making the lithium-ion battery system also more expensive than the heat storage system.

In the future it would be beneficial to study these systems more to determine their long-term efficiency and total environmental effects. Some research ideas include a study on the effects of weather conditions and different seasons, a study of the environmental effects the manufacturing of the system components may possibly have and a study on the technology and price development of the components. It would also be beneficial to research different possibilities to solve the problem of energy insufficiency during the moments of no available solar energy.

Keywords: trigeneration, heat storage, lithium-ion battery, organic Rankine cycle (ORC), absorption chiller

TIIVISTELMÄ

Nina Olenius: Kolmoistuotannon tarkastelu korkean lämpötilan lämpövaraston yhteydessä
Diplomityö
Tampereen yliopisto
Ympäristö- ja energiatekniikka
Kesäkuu 2022

Nyt kun maailma on pikkuhiljaa siirtymässä pois fossiilisista polttoaineista energian tuotannossa, ratkaisujen löytämisestä sähköverkon vakauden säilyttämiseksi on tullut tärkeää, sillä uusiutuvat energian lähteet eivät ole aina saatavilla. Energiavarastot tarjoavat yhden ratkaisun tähän ongelmaan ja ehkä tunnetuimpia energiavarastoja ovat akut. Akkujen ongelma on kuitenkin niiden hinta, joka on erittäin korkea erityisesti suuremmilla akuilla. Vaihtoehto akuille voisi olla lämpövarasto, jossa energia on varastoitu lämmön muodossa.

Energiavarastot mahdollistavat täysin erilaisen tavan ohjata omaa energian kulutusta. Ne mahdollistavat itsenäisemmän energian tuonnin ja tarjoavat mahdollisuuden sähköverkon ulkopuolisiin ratkaisuihin. Energiavarasto voi yleensä vastata vain yhden energiamuodon tarpeeseen kerrallaan, ellei sitä ole yhdistetty muihin järjestelmiin, kuten lämmitysvastuksiin.

Tämän diplomityön tarkoituksena oli tutkia kolmoistuotantoa ja sen käyttökohteita sekä vertailla kahta eri kolmoistuotantoa hyödyntävää järjestelmää. Järjestelmät, joita työssä tutkittiin, olivat lämpövarastojärjestelmä, joka hyödyntää orgaanista Rankine-kiertoa sekä absorptiojäähdytintä, sekä litiumioniakkujärjestelmä, joka hyödyntää lämpöpumppua. Kolmoistuotanto on energiantuotannon tapa, jossa sähkö, lämpö ja kylmä tuotetaan yhtäaikaisesti. Lämpövarastojärjestelmässä sähkö tuotetaan orgaanisessa Rankine-kierrossa, kun taas lämpö ja kylmä on tuotettu absorptiojäähdyttimellä. Litiumioniakkujärjestelmässä sähkö otettiin suoraan sähköakusta ja lämpö ja kylmä tuotettiin lämpöpumpulla.

Molempien järjestelmien tekniikoita tutkittiin ja järjestelmille toteutettiin Excel-simulointi, jonka tarkoituksena oli tutkia niiden toimintaa tietyssä toimintaympäristössä. Molemmille järjestelmille toteutettiin myös kustannusanalyysi. Simulointi toteutettiin kolmelle eri tapaukselle: normaalille aurinkoiselle päivälle, pilviselle päivälle sekä päivälle, jolloin aurinkoenergiaa ei ole lainkaan saatavilla. Käyttökohteeksi valikoitui sairaala. Muita mahdollisia käyttökohteita olisivat olleet esimerkiksi hotelli, toimistorakennus tai yliopisto. Tulokset näyttivät, että molemmat järjestelmät suoriutuivat yhtä hyvin simulaatiosta. Ne pystyivät vastaamaan sairaalan energian tarpeeseen kahdessa ensimmäisessä laskentatapauksessa mutta kolmannessa tapauksessa, jossa aurinkoenergiaa ei ollut lainkaan saatavilla, varastojen energia loppui ennen puoltapäivää. Suurempi ero järjestelmien välille löytyi kustannusanalyysista. Järjestelmien pääkomponenttien investointikustannukset jaettiin niiden käyttövuosille annuiteettimenetelmän mukaisesti. Analyysin tulokset osoittivat, että litiumioniakku on kaikista kallein komponentti tehden siitä myös kalliimman järjestelmän kuin lämpövarastojärjestelmästä.

Tulevaisuudessa olisi hyödyllistä tutkia näitä järjestelmiä lisää, jotta voitaisiin selvittää niiden pidemmän aikavälin tehokkuus sekä kokonaisympäristövaikutukset. Muutamia mahdollisia tutkimuskohteita voisivat olla vuodenaikojen ja sääolosuhteiden vaikutus järjestelmien toimintaan, järjestelmäkomponenttien valmistamisesta mahdollisesti aiheutuvat ympäristövaikutukset sekä komponenttien teknologia- ja hintakehitys. Hyödyllistä olisi myös tutkia erilaisia mahdollisuuksia ratkaista energian riittämättömyyden aiheuttama ongelma hetkinä, jolloin aurinkoenergiaa ei ole saatavilla.

Avainsanat: kolmoistuotanto, lämpövarasto, litiumioniakku, orgaaninen Rankine-kierto (ORC), absorptiojäähdytin

PREFACE

This thesis concludes my studies of Energy Engineering at Tampere University. I would like to thank Polar Night Energy for providing me with such an interesting topic to work on. Special thanks to Ville Kivioja for guiding me through this process.

I would also like to thank University Lecturer Henrik Tolvanen for his guidance and feedback on my thesis as well as all the great lectures I had the pleasure to attend to. Equally, I would like to give thanks to Principal Lecturer Aki Korpela for sharing his viewpoint on the thesis and guiding me in the world of electrical engineering.

Thank you to my family for supporting me through my studies and my friends for making the studying fun. Finally, I want to give thanks to my other half, Erhan, for standing by my side and being the rock that I needed in my life. Thank you for pushing me to finish my thesis and tolerating me when my stress levels were sky high.

Tampere, 12.6.2022

Nina Olenius

TABLE OF CONTENTS

LIST OF FIGURES

LIST OF TABLES

LIST OF SYMBOLS AND ABBREVIATIONS

AACE	*Association for the Advancement of Cost Engineering*
CAPEX	*capital expenses*
CCHP	*combined cooling, heating, and power*
CHP	*combined heat and power*
COP	*coefficient of performance*
HFO	*hydrofluoroolefin(s)*
HTF	*heat transfer fluid*
Li-ion	*lithium-ion*
LMTD	*logarithmic mean temperature difference*
OPEX	*operational expenses*
ORC	*organic Rankine cycle*
SOFC	*solid oxide fuel cell*
SRC	*steam Rankine cycle*
TES	*thermal energy storage*
UPS	*uninterrupted power supply*

A	heat transfer area	m^2
A_{inv}	annual investment costs of a system	€ a^{-1}
A_{oper}	annual operational costs of a system	€ a^{-1}
C	costs of a facility	€
$c_{n/i}$	annuity factor	-
g	gravitational acceleration	m s^{-2}
h	enthalpy	J kg^{-1}
i	imputed rate of interest	-
$\dot{m}$	mass flow	kg s^{-1}
$\dot{m}_0$	maximum mass flow at the maximum pressure	kg s^{-1}
n	economic lifetime	years
P	annual costs of a system	€ a^{-1}
$P_{inv,tot}$	total investment costs of a system	€
p_α	choking pressure	bar
$p_{\alpha 0}$	maximum pressure	bar
p_ω	final pressure of expansion	bar
$p_{\omega 0}$	minimum pressure of expansion	bar
Q	capacity of a facility	W
$\dot{Q}$	heat transfer rate	W
$\dot{Q}_{cond}$	heat removed from a system	W
$\dot{Q}_{evap}$	heat absorbed to a system	W
T	temperature	K, °C
T_{lm}	logarithmic mean temperature	-
U	overall heat transfer coefficient	W m^{-2} K^{-1}
v	velocity	m s^{-1}
W	work	W
x	scale factor	-
z	height	m

1. INTRODUCTION

The energy production system has changed drastically over the decades. New energy sources have been harnessed and the global energy consumption has grown. Energy demand keeps growing around the world as the standard of living keeps getting better and people become wealthier. Energy consumption will keep on growing unless energy efficiency is improved. The growing energy consumption creates a challenge for the change away from fossil fuels as the low- and zero-carbon energy sources must meet the energy demand while displacing the fossil fuels. (Ritchie, Roser and Rosado, 2020)

Trigeneration research field is quite wide. Fong and Lee (2017) studied the effects of different climate conditions on trigeneration. They found, that the trigeneration system performed better in climate conditions that have a stable need for heating and/or cooling. Climates with cold winters and hot summers or a year-around summers are the most convenient for trigeneration, while in temperate climates, trigeneration may not reach its full potential. (Fong and Lee, 2017) In addition to climate conditions, operating strategies are a defining factor for trigeneration. Mago and Hueffed (2010) studied a trigeneration system under three different operating strategies: based on electricity demand, based on thermal demand and based on seasonal alteration. Their research found, that trigeneration can reduce the operational costs of a facility under all three operating strategies when compared to conventional energy production technologies. (Mago and Hueffed, 2010)

Another topic for research has been the system configuration for trigeneration. The system configuration differs based on the primary energy source. Al-Sulaiman, Dincer and Hamdullahpur (2013) studied three trigeneration systems: biomass-trigeneration, solar-trigeneration and solid-oxide-fuel-cell (SOFC) trigeneration. Solar-trigeneration has also been researched by Jafary et al. (2021) and Buonomano et al. (2015), who studied a system powered by solar and geothermal energy. SOFC-trigeneration has been studied by Chen and Ni (2014), who studied the system for hotel applications.

In this thesis a techno-economic analysis on trigeneration system utilizing a heat storage is performed. The purpose of this thesis is to study trigeneration combined with a high temperature heat storage. The study is done from both technical and economical point of view. Since this kind of combination is rather new and has not been studied widely,

there is interest to compare it with a more commonly known technical solution. The system to which trigeneration system is compared to is a lithium-ion battery-heat pump system; a system whose technical abilities and economic feasibility are well known. This thesis' focus is on the trigeneration process and its functionality in certain case conditions presented later. Thus, this thesis does not focus on the functionality of a heat pump and its functionality is examined on a very basic level in the calculations. Solar panels are also considered only for their energy production and are presumed to execute in a well enough manner for the purposes of this thesis. These limitations are done to ensure the focus stays on the trigeneration process and keep the thesis from expanding too far.

The research methods in this thesis combine literature review, a simulation of trigeneration systems and an economic feasibility analysis. The simulation is performed on Microsoft Excel with CoolProp for Excel expansion.

The research questions in this thesis are:

1. What are the applications to which trigeneration is suitable for?
2. Which combination of technologies can best be applied with high temperature heat storage?
3. What are the production values, respectively for power, heating, and cooling, for the chosen application and trigeneration production?
4. How does the chosen combination of technologies with a heat storage compare to the chosen competing trigeneration technology in terms of production values and economic feasibility?

Trigeneration and its applications are presented in chapter 2. This chapter goes deeper into trigeneration and its advantages as well as the possible applications where trigeneration could be utilized. Chapter 3 introduces the different technologies used in the simulation. In this chapter the functionality of these technologies is explained keeping the focus on the important details considering trigeneration. Finally in chapter 4, the trigeneration process with a heat storage and the competing trigeneration process with a lithium-ion battery are presented in detail. The initial values and the base for the economic feasibility analysis are also presented in this chapter. Simulation results for both systems are presented in chapter 5. This chapter also immerses into the differences in these systems, compares their performance based on the results and presents suggestions for future research. Finally, chapter 6 concludes this thesis.

2. TRIGENERATION AND ITS APPLICATIONS

This chapter gives an overview of trigeneration, its working principles, benefits, and its potential primary energy sources. It also presents the requirements for the utilization of trigeneration. Based on these requirements, some suitable applications are presented along with applications that are already in use.

2.1 Trigeneration overview

Trigeneration, also known as combined cooling, heating, and power (CCHP), is an energy production method that produces heat, electricity, and cooling simultaneously from one energy source. Trigeneration systems can be classified by three characteristics: the size of the plant, the sequence of energy used, and the type of prime mover. Naturally the size of the plant depends on the application and the needed power, but a rough grouping could be large scale (1 MW_e onward), small scale (60 kW_e–1.5 MW_e) and micro systems (less than 50 kW_e). When classified by the sequence of energy, the systems are grouped by their energy production priority. This means, that systems, whose priority is to produce electricity, are topping cycle systems, and systems, whose priority is to produce heat, are bottoming cycle systems. A prime mover provides the mechanical motive power for the trigeneration system. Some examples of prime movers are steam and gas turbines, reciprocating internal combustion engines, and organic Rankine cycle. (Al Moussawi, Fardoun and Louahlia-Gualous, 2016) Figure 2.1 presents an example of a trigeneration system and its working principle.

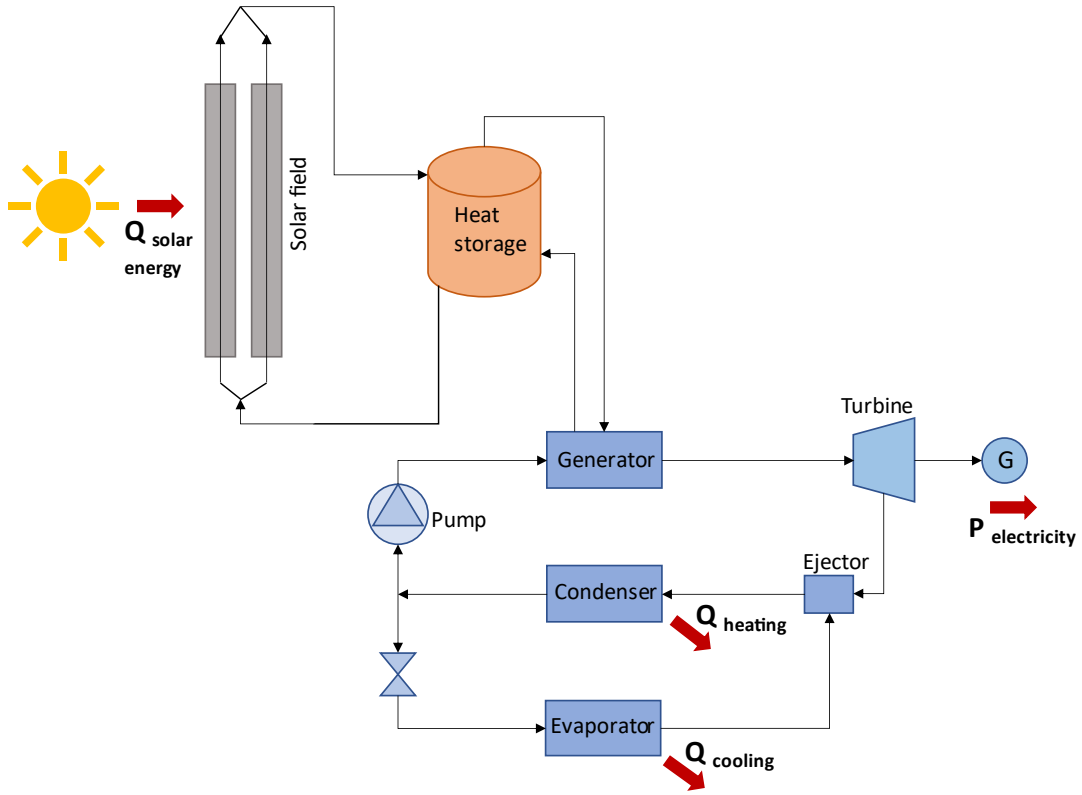

Figure 2.1 *An example of a trigeneration process. Modified from* (Bellos and Tzivanidis, 2018b)

In Figure 2.1 process chart the primary energy source is solar energy, which is produced with parabolic trough collectors. These collectors are coupled with a storage tank, where the heat storage medium is layered according to the temperature. From the bottom of the tank, the medium with lower temperature exits back to the solar collector field. From the top of the tank, the medium with higher temperature enters to a generator, from where it returns to the tank after releasing heat to superheated vapor. The vapor is then lead to a turbine, which is coupled with an electrical generator to produce electricity. After the turbine, the vapor enters a condenser via an ejector. The condenser produces heat. When the vapor leaves the condenser, it is saturated liquid, and it is separated into two streams. One goes back to generator and the other enters to an evaporator, where the cooling is produced. From the evaporator the now saturated vapor enters to the ejector, where the two streams (one from the turbine and the other from the evaporator) are mixed. (Bellos and Tzivanidis, 2018b)

Trigeneration has many advantages compared to traditional power plants or combined heat and power (CHP) -systems. One of those is lower fuel consumption, which reduces annual operational costs (OPEX) leading to shorter payback time. The ability to operate with several fuels and the possibility to integrate renewables increase energy reliability,

make production on-site possible and allow for energy standards to be met. Overall efficiencies are also higher (Al Moussawi, Fardoun and Louahlia-Gualous, 2016; Shi, Liu and Fang, 2017) for example, a trigeneration system can achieve as much as 50 % higher overall efficiency than a same size CHP plant (Shi, Liu and Fang, 2017). The downside of trigeneration, though, is that it is only profitable if all three energy forms are needed (Ziher and Poredos, 2006).

The primary energy source for trigeneration partly determines the system configuration. For example, a SOFC-trigeneration system requires multiple blowers, an inverter, an after burner and pumps and heat exchangers for the energy to be in right form for the next part of the process while biomass-trigeneration only requires a biomass combustor and a cyclone. (F. A. Al-Sulaiman, Dincer and Hamdullahpur, 2013) A trigeneration system is not limited to one primary energy source per system. A geothermal-solar trigeneration system uses the different primary energy sources to produce different end products. Solar energy is mainly used for electricity production while geothermal energy is used for cooling and heating production. (Buonomano *et al.*, 2015)

2.2 Suitable applications

The feasibility of trigeneration system requires a high consumption of heating, cooling and electrical energy throughout the year (Ziher and Poredos, 2006). Such places are e.g., hospitals, hotels, office buildings, schools or universities and apartment buildings. In trigeneration system the production of heating and cooling requires insulation to keep the temperatures at a needed stage and to keep the thermal energy production as a valuable benefit. This means, that the trigeneration systems are mostly used as decentralized systems, and thus they are located near the end user. (F. Al-Sulaiman, Dincer and Hamdullahpur, 2013)

Table 2.1 shows the energy consumption by sector in three countries. The countries were chosen to represent different kinds of climate conditions.

Table 2.1. *Energy consumption per capita per year by sector in Finland, Germany, and Morocco in 2019. Modified from* (*IEA – International Energy Agency*, 2021)

Country	*Electricity*		*Heating*		*Cooling*	
	Residen-tial [MWh]	Commer-cial [MWh]	Residen-tial [MWh]	Commer-cial [MWh]	Residen-tial [kWh]	Commer-cial [kWh]
Finland	4.07	3.23	6.49	2.89	20.09	-*
Germany	1.52	1.59	5.24	1.96	15.03	41.42
Morocco	0.31	0.16	0.03	0.01	2.26	8.28

*No information was provided in the source.

As can be seen from the table, both electricity and heat consumption, are higher in colder climate conditions than in warmer climate conditions. What is surprising though, is that the use of cooling is also higher in Finland than in Germany or Morocco. The low numbers of Morocco could be explained by general lower standard of living.

According to Bawaneh et al. (2019) 10.3 % of the total energy consumption in commercial sector was used by healthcare facilities in the United States. This accounts to 210.42 billion kWh of energy and 63 % of this energy is utilized in heating, water heating, ventilation and cooling (Bawaneh *et al.*, 2019) Table 2.2 presents a breakdown of energy consumption per square meter by end use type.

Table 2.2 *Overall healthcare energy consumption per year. Modified from* (Bawaneh *et al.*, 2019)

End use type	*Energy usage [kWh/m^2]*
Space heating	163
Cooling	62
Ventilation	62
Water heating	62
Lighting	46
Cooking	64
Refrigeration	14
Office equipment	13
Computers	26
Other	64

When the end use types are divided into electricity, heating, and cooling, it can be seen that the energy form hospitals mostly use is electricity. Heat is used for space and water heating while cold is only used for cooling. Figure 2.2 gives a visual representation of how the three are divided in hospitals.

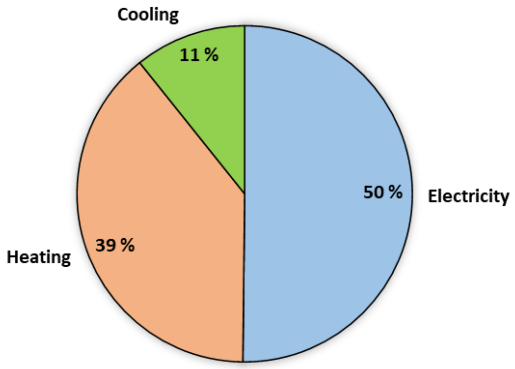

Figure 2.2 *Energy division in hospitals.*

A hotel is another possible application for trigeneration. Unlike hospitals, hotels do not run on full power 24 hours a day and seven days a week. A small hotel in Finland uses 1,900 MWh of electricity and 927 MWh of heating energy in a year (Tyrjy, Aquarius and

Hiittenharju, 2009). The annual energy consumption of Italian hotels is presented in Table 2.3. In the table a small hotel has 60 rooms, a medium hotel has 150 rooms, and a large hotel has 300 rooms.

Table 2.3 *Annual energy consumption in Italian hotels. Modified from* (Bianco *et al.*, 2017)

End use type	*Small hotel*	*Medium hotel*	*Large hotel*
Winter heating [MWh]	150–210	375–525	750–1,050
Hot sanitary water [MWh]	228–264	570–660	1,140–1,320
Summer air conditioning [MWh]	60–210	150–525	300–1,050
Electricity consumption [MWh]	300–660	750–1,650	1,500–3,300

The small hotel in Finland uses roughly as much electricity as a large hotel in Italy and as much heating as a medium hotel in Italy. The greater heating consumption values of Finland can be explained by the colder climate, but the electricity consumption is trickier. One explanation is always a difference in measurement techniques. When the end use types of Italian hotels are divided into electricity, heating and cooling, there are two possible scenarios depending on which value is chosen. Figure 2.3 gives a visual representation on the energy division for both scenarios. A) is for smaller energy consumption value and B) is for the greater energy consumption value.

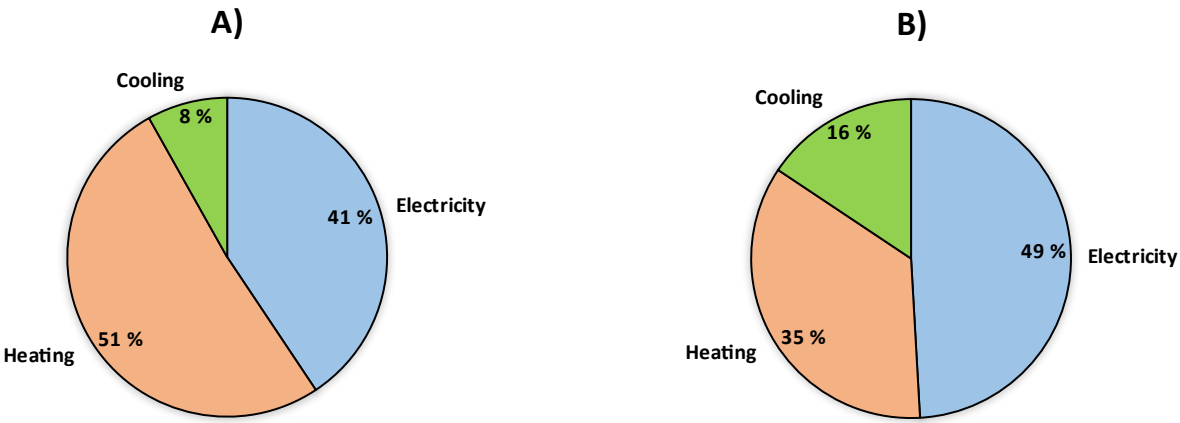

Figure 2.3 *Energy division in hotels. A) for smaller energy consumption B) for greater energy consumption.*

As can be seen from Figure 2.3, when energy consumption rises, the consumption of electricity and cooling rise while the consumption of heating decreases. The energy division as a whole though is similar to energy division in hospitals.

In addition to hospitals and hotels, trigeneration has been utilized with other subjects as well. A greenhouse in Iran was combined with a solar trigeneration system to provide heating during winter and cooling during summer. The trigeneration system was able to save water and fuel in comparison to a conventional greenhouse, where heating is produced with a gas heater and cooling with a pad-fan. (Mohsenipour *et al.*, 2020) The heating load of an office building mainly consists of space heating. As working places, the electricity demand of an office building consists of electric office equipment, lighting, elevators, auxiliary chillers, and other cooling equipment. Even though the electricity, heating and cooling demands are rather stable during the office hours, they become quite low during non-office hours and holidays. (Fong and Lee, 2017) According to Mago and Hueffed (2010), trigeneration can reduce the operational costs, primary energy consumption as well as the CO_2 emissions of an office building. However, the profitability energy wise depends on the stability of the energy demand (Fong and Lee, 2017). The energy demand of a university campus in China was covered with a trigeneration system. The campus consists of teaching building, library building, office building, dormitory, and commercial building. The energy demand of the university campus varies a lot between winter and summer. (Jiang *et al.*, 2016) Winters are cold and summers are hot, where the university campus is located (Jiang *et al.*, 2016), which is ideal for a trigeneration system (Fong and Lee, 2017).

3. TECHNOLOGIES USED FOR TRIGENERATION

This chapter presents the different technologies, which are used in the heat storage system and in the lithium-ion battery (Li-ion battery) system. Heat storage, absorption chiller and Organic Rankine Cycle turbine (ORC) are part of the heat storage system while heat pump and lithium-ion battery are part of the competing system. The system components are presented in Figure 3.1 where a) is the heat storage system and b) is the Li-ion battery system. Both systems are charged with renewable energy.

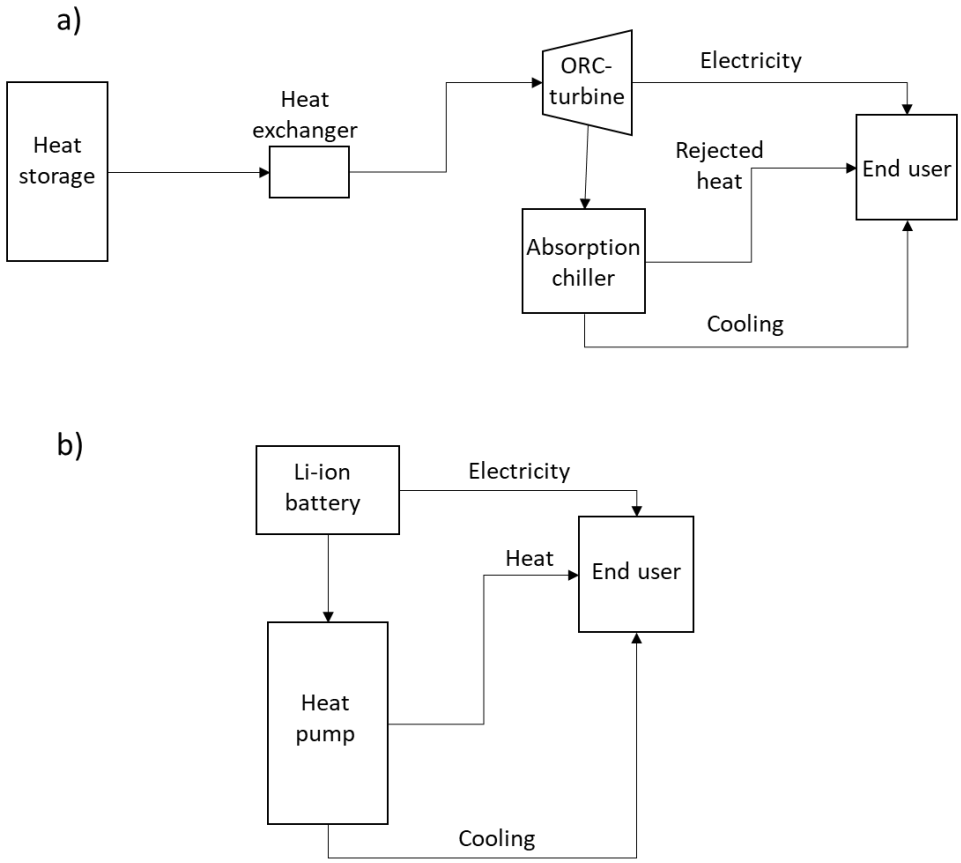

Figure 3.1 *Trigeneration system components for two different configurations.*

3.1 Heat storage

The intermittent nature of renewable energy sources presents a challenge in balancing the consumer demand and the energy availability. An energy storage provides a solution for this problem by shifting excess energy from high-insolation periods to times when renewable energy is not available. This does not only make the whole power system more efficient but also more reliable and flexible. A common example of energy storage is a battery, which stores energy in chemical form. The main drawbacks of commercial

batteries are their price and limited lifetime. A heat storage or thermal energy storage (TES) could provide an alternative solution for the energy storage problem. TES is cheaper than commercial batteries and it stores energy in thermal form, which makes it possible to utilize energy sources from larger scale. TES usually also has a longer usable lifetime, and it comes in many varieties expanding its usability even more. (Macchi and Astolfi, 2017, pp.591)

TES is temporary storage, where energy is stored in high or low temperature. Thermal energy can be stored by altering its sensible or latent heat or by a combination of these two. Altering sensible heat means that the temperature of a substance is either elevated or lowered and altering latent heat means that the phase of a substance is changed. Sensible heat changes are dependent on the specific heat capacity of the substance as well as temperature change. The change in latent heat differs from sensible heat changes in occurring at a constant temperature. Because of this difference, the storage systems utilize different storage mediums. (Dinçer and Rosen, 2010) Sensible heat storage systems can use, for instance, water, earth materials and thermal oils while latent heat storage systems can use phase change materials from larger scale, such as alcohols, paraffin and salts. (Dinçer and Rosen, 2010, p. 76; Alva, Lin and Fang, 2018)

Storage mediums used in sensible heat storages store the heat in their specific heat capacity (Dinçer and Rosen, 2010). This is one of the reasons why water is a good storage medium for sensible heat systems. Its specific heat capacity is 4.184 kJ/kgK. Other advantages of water are its non-toxicity, easy availability, and cheap cost. Water can be used in all its forms, which makes water suitable for many applications with different process requirements. Downside of water as storage medium is its corrosiveness and high vapor pressure. Thermal oils have lower specific heat capacity than water (≈ 2 kJ/kgK) but they have other advantages over water. Thermal oils remain in liquid phase at higher temperatures, and they have lower vapor pressure. Thermal oils can also cause corrosion, when used above their operating temperature range, due to oxidation and thus carbolic acid, peroxide compounds etc. formation. Thermal oils are the most used heat transfer fluids (HTF) for sensible heat storage systems using earth materials as fillers in storage tank. These earth materials such as rocks, sand, and gravel work as a storage medium and heat transfer surface at the same time, which reduces the need for heat exchangers. The costs of earth materials are low and they are easy to access, non-toxic and also non-flammable. (Alva, Lin and Fang, 2018)

For latent heat storage systems, the situation is different for the storage mediums store the heat in their latent heat while going through a phase change at constant temperature (Dinçer and Rosen, 2010). Solid–liquid phase changes are common as well as solid–

solid changes though the latent heat is less. With liquid–gas change the latent heat is the greatest, but the huge volume growth is a problem. The most used organic storage medium with commercial latent heat systems is paraffin. Paraffins from n-pentadecane to n-triacone are usually used in TES applications. The advantages from using paraffin are, for instance, its chemical stability, compatibility with metal containers and being odourless. Downsides then are low density, low thermal conductivity, and large volume change during phase change. Sugar alcohols are another storage medium used with latent heat systems. They are suitable to be used at temperature range 90–250 °C, they are non-toxic and have low costs. Alcohols show polymorphism, which can cause problems in TES applications. Salts are suitable for high temperature TES for they have high melting points. Salts are of different types and therefore not all are suitable to be used as a storage medium. Inorganic salts, for example, have low thermal conductivity. (Alva, Lin and Fang, 2018)

Both sensible and latent heat storages have their advantages and disadvantages. Latent heat storage has higher energy storage density due to latent heat being 50–100 times larger than sensible heat. Phase change materials are non-toxic in general, but they have low thermal conductivities. The outlet temperature of HTF in latent heat systems is constant when in sensible heat systems the HTF temperature starts to gradually decrease. Sensible heat storages mediums perform well at high temperatures and hence are suitable for high temperature TES applications. For most part the mediums are also cheap. (Alva, Lin and Fang, 2018)

The quality of the energy should be taken into consideration, when talking about TES. For instance, one kWh of energy can be stored either in 10 kg of water at the temperature of 86 °C or in 1,000 kg of water at the temperature of 0.86 °C. For many engineering applications the former is a more attractive option due to higher temperature and smaller volume. In general, temperature is one of the determining factors when it comes to the potential applications for a heat storage. (Dinçer and Rosen, 2010)

3.2 Absorption chiller

Absorption chillers are used to generate the cold in a trigeneration process. They differ from compression chillers by utilizing heat instead of electricity as an energy source. (Chen and Ni, 2014) The fluid circling the absorption chiller consist of a refrigerant and an absorbent (Le Lostec, Galanis and Millette, 2013). The most widely used fluids are water-ammonia and lithium bromide-water (LiBr-H_2O) mixtures (Chen and Ni, 2014). In water-ammonia mixture, the refrigerant is ammonia and the absorbent is water unlike in

LiBr-H_2O mixture, where water works as a refrigerant and lithium bromide as the absorbent (Le Lostec, Galanis and Millette, 2013). These two fluids are used in different applications for they have different qualities in providing cold. Water-ammonia is often used in food refrigeration applications because it can provide temperatures below freezing point. LiBr-H_2O mixture on the other hand suits well the needs of building air-conditioning, since it is able to lower the temperature of water to 4–38 °C. Absorption cycle consists of condenser, evaporator and expansion valve. (Chen and Ni, 2014)

Figure 3.2 presents the process inside the absorption chiller. Heat (Q_G) is injected into generator at higher temperature (T_G). The generator contains LiBr-H_2O mixture, which then starts to free water at high pressure (p_C). As water is freed from the mixture, the mixture becomes rich in LiBr. The now high-pressure and high-temperature water vapor moves to the condenser, where it condenses back to liquid form by releasing heat (Q_C) to its surroundings. This high-pressure liquid form water is led through either an expansion valve or a throttling device to decrease the pressure (p_E) to the level of the evaporator. When the water enters the evaporator, it is in a state of saturated liquid or wet vapor. In the evaporator, it absorbs heat (Q_E) from its surroundings and therefore fully evaporates, which produces the wanted effect of cooling and maintains a low temperature (T_E). Next, the now saturated or superheated water vapor enters the absorber at the evaporator pressure. The rich LiBr liquid mixture in the generator is brought to the absorber through an expansion device to bring down its pressure. In the absorber, the rich LiBr liquid mixture absorbs the saturated or superheated water vapor making it a lean LiBr liquid mixture. The absorption process is exothermic, so the generated heat (Q_A) is removed to the environment. Eventually, the lean LiBr liquid mixture is led back to the generator. Because the pressure at the generator is higher than at the absorber, the LiBr lean liquid mixture is first pumped to the right pressure (p_C). (Tyagi *et al.*, 2018)

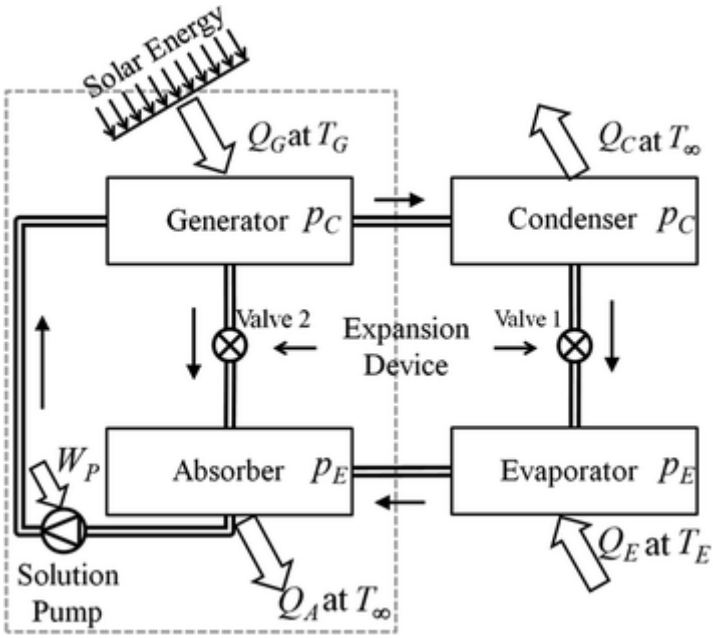

Figure 3.2 *Process description in absorption chiller. (Tyagi et al. 2018)*

3.3 Organic Rankine Cycle

When dealing with low temperature heat sources and/or limited available thermal power, such as heat storages, it becomes attractive to utilize another type of prime movers, such as ORC, says Macchi et al. (2017 pp. 3). ORC is similar to Steam Rankine Cycle (SRC) in terms of technical implementation. In both processes a high-pressure liquid is vaporized and the vapor is expanded to a lower pressure, which releases kinetic energy. To close the cycle, the now low-pressure vapor is condensed and pumped back to higher pressure. The components needed for the former process are, in order, a boiler or an evaporator, a turbine, a condenser and a pump. The difference between ORC and SRC is the working fluid, which is water for SRC and an organic compound for ORC. (Quoilin *et al.*, 2013) The working fluids for ORC can be classified into HTFs, brines, humid air, molten salts, pure working fluids, and mixtures of fluids as the working fluid. For example, brines are suitable for geothermal systems and molten salts for solar power tower systems. Pure working fluid, such as n-pentane or hydrofluoroolefins (HFO), means, that the fluid experiences no temperature change when it changes phase at constant pressure. (Macchi and Astolfi, 2017, pp.92) The benefit of organic compounds as the working fluid is their lower boiling point, which allows for power generation from low heat sources (Quoilin *et al.*, 2013).

Because of the possibility to use other substances than water as the process medium, ORC can utilize low temperature heat sources. Operating conditions and the efficiency of the system depend on the selection of the process medium. (Wang *et al.*, 2013) The

temperature of the heat source is significant in choosing the optimal process medium for the process. For example, with heat source temperature of 47 °C the optimal process medium would be R143a and with heat source temperature of 227 °C the optimal process medium would be R123. (Tocci *et al.*, 2017) Critical temperature determines the maximum evaporating temperature level for a subcritical cycle, which makes it an extremely significant parameter for the process medium. Toluene, for instance, has a critical temperature of 318.6 °C and a critical pressure of 41.26 bar. (Bellos and Tzivanidis, 2018a) Figure 3.3 presents the Ts-diagram for toluene.

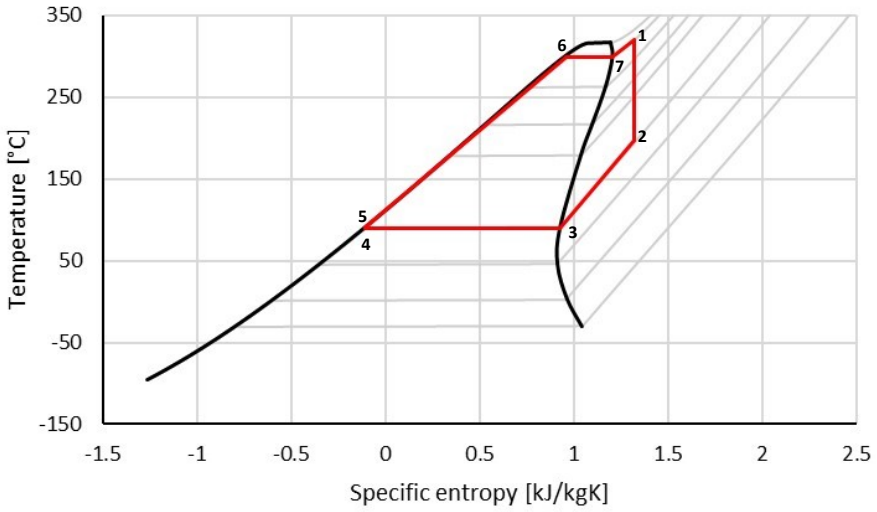

Figure 3.3 *Ts-diagram for toluene with an ORC.*

As can be seen from Figure 3.3 toluene has wide range temperature wise. The red cycle represents an organic Rankine cycle, where toluene is the process medium. The maximum temperature then is around the critical temperature while the minimum temperature is around 90 °C.

ORC has a few advantages compared to other power producing cycles. The process is economical, and it does not require an additional fuel. In addition to that the environmental impacts of ORC are low just like the maintenance costs. However, the energy conversion efficiency being around 8–12 %, creates a challenge for ORC. (Pethurajan, Sivan and Joy, 2018) To achieve the best possible efficiency, it is crucial to select the working fluid well (Cotana *et al.*, 2014). Because of this, it is important to estimate the thermodynamic and transport properties of the working fluid, determine the heat transfer rate in the evaporator as well as the condenser and model the expansion machine with complexities of a two-phase fluid. (Pethurajan, Sivan and Joy, 2018)

The turbines used in ORC systems and in SRC systems are essentially the same. Axial turbines work well in systems with high flow rates and low-pressure ratio while radial

turbines are the opposite and work well with low flow rates and high-pressure ratios. Low flow rates and high-pressure ratios means that the temperatures are also lower and thus radial turbines are preferred for ORC systems. With higher temperatures, axial turbine may be preferred for the cooling of the turbine blades is easier with axial turbine. (Pethurajan, Sivan and Joy, 2018)

Aurelian Stodola's cone law also known as the law of the ellipse can be used to define the mass flow through a turbine at a certain choking pressure when the inlet and outlet pressures of the turbine are known. The Stodola equation is defined as follows

$$\frac{\dot{m}}{\dot{m}_0} = \frac{p_\alpha}{p_{\alpha 0}} \sqrt{\frac{1 - (p_\omega / p_\alpha)^2}{1 - (p_{\omega 0} / p_{\alpha 0})^2}}\,, \tag{1}$$

where $\dot{m}$ is the mass flow corresponding to the choking pressure p_α, $\dot{m}_0$ is the maximum mass flow corresponding to the maximum pressure $p_{\alpha 0}$, p_ω is the final pressure of the expansion and $p_{\omega 0}$ is the minimum pressure to which the turbine can expand. (Fuls, 2017)

3.4 Heat exchanger

Heat exchangers transfer heat between two or more fluids that flow through the exchanger. Flow configuration is an important characteristic in heat exchanger design. Flow configuration is the geometric way the different streams are set according to each other. The different flow configurations are counter flow, parallel flow, cross flow, cross counter flow and multipass shell and tube. (Hewitt, 1990, pp. 1.1.1 1) The best-known flow configurations are counter and parallel flow configurations. They are symmetrical and the mean temperature difference is determined as the logarithmic mean of the local temperature differences. (*VDI Heat Atlas*. 2nd ed. 2010., 2010, pp. 38)

To determine the logarithmic mean temperature, first it is important to determine the local temperature differences at both ends of the heat exchanger. The local temperature differences for counter flow are as follows

$$\Delta T_1 = T_{hot,in} - T_{cold,out} \tag{2}$$

$$\Delta T_2 = T_{hot,out} - T_{cold,in} \tag{3}$$

where T_{hot} refers to the temperature of the fluid releasing heat and T_{cold} refers to the temperature of the fluid receiving heat. Subindexes in and out refer to the direction of the flow in relation to the heat exchanger. For parallel flow, the local temperature differences are defined

$$\Delta T_1 = T_{hot,out} - T_{cold,out} \tag{4}$$

$$\Delta T_2 = T_{hot,in} - T_{cold,in} \tag{5}$$

where, like with counter flow, T_{hot} refers to the fluid releasing heat and T_{cold} refers to the fluid receiving heat. Subindexes in and out refer to the direction of the flow in relation to the heat exchanger. (*VDI Heat Atlas*. 2nd ed. 2010., 2010, pp. 38) A visual representation of the local temperature differences is presented in Figure 3.4.

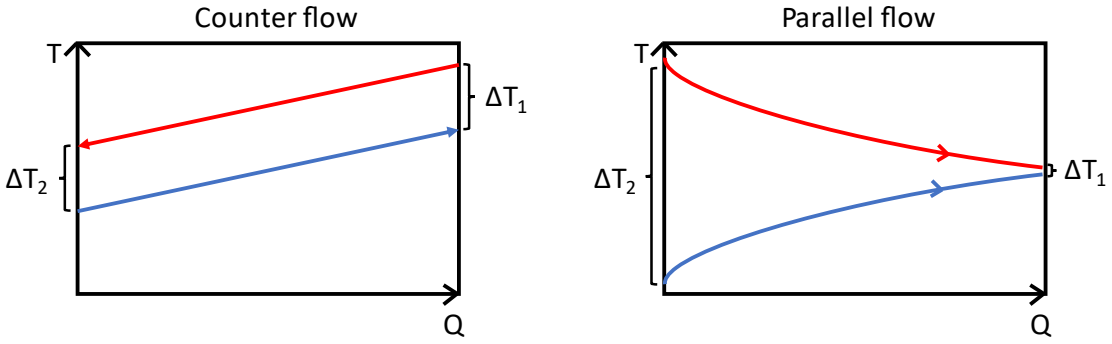

Figure 3.4 *Local temperature differences in counter and parallel flows.*

The logarithmic mean temperature is then defined as (*VDI Heat Atlas*. 2nd ed. 2010., 2010, pp. 38)

$$\Delta T_{lm} = \frac{\Delta T_2 - \Delta T_1}{\ln \frac{\Delta T_2}{\Delta T_1}} \tag{6}$$

When calculating the heat transfer rate over the heat exchanger and using the logarithmic mean temperature as the temperature difference, the heat transfer rate is determined

$$\dot{Q} = UA\Delta T_{lm} \tag{7}$$

where U is an overall heat transfer coefficient, A is the area of the heat exchanger and ΔT_{lm} is the logarithmic mean temperature as defined above in equation 6. (Serth, 2007, pp. 93)

Counter flow heat exchangers are the most efficient. They utilize the available temperature difference best and thus can obtain the biggest temperature change in the fluids. Parallel flow heat exchanger on the contrary fails to utilize the temperature difference well. (Hewitt, 1990, pp. 1.1.1 1-2)

When estimating the performance of a heat exchanger, it is important to know the flow configuration, flow rates and what the resistances to heat transfer are.

Energy equation for a steady flow heat exchanger is determined as

$$\dot{m}\Delta\left(h + \frac{v^2}{2} + g_n z\right) = \dot{Q} - \dot{W}_s, \tag{8}$$

where $\dot{m}$ is the mass flow rate of the flow, Δ is the change in energy (enthalpy, kinetic energy, and potential energy), $\dot{Q}$ is the heat transfer rate into the studied area and $\dot{W}_s$ is the work transferred to the outside by a rotating shaft. With many applications kinetic and potential energy can be assumed to be 0 as well as the shaft work. (Hewitt, 1990, 1.2.1 1) When only the mass flow rate, enthalpy change and the heat transfer rate are considered and there are two streams flowing through the heat exchanger, the energy equation changes into

$$\dot{m}_1\left(h_{1,out} - h_{1,in}\right) + \dot{m}_2\left(h_{2,out} - h_{2,in}\right) = 0 \tag{9}$$

where the subindexes 1 and 2 refer to the different streams. (Hewitt, 1990, 1.2.4 1)

3.5 Heat pump

The primary task of a heat pump is to produce heat. The temperature of the heat produced with the heat pump must be at the right level for its application in order that the heat can be used. Each application has its own temperature range, and they are presented in Table 3.1. (Aittomäki and Aalto, 2012, pp. 336)

Table 3.1 *Temperature ranges of heat pump applications* (Aittomäki and Aalto, 2012, pp. 336)

Application	*Temperature range [°C]*
Air heating of buildings	20–40
Water heating of buildings	30–80
Heating of domestic water	50–80
District heating	70–120
Steam development	110–150
Process applications	30–

In this system the applications of interest are air and water heating of buildings and heating of domestic water. Pumping of heat can be executed in several ways though compression machinery is especially interesting for this case. Compressor driven steaming machinery is based on Clasius-Rankine -process and it uses mechanical machinery. The structure and operation are the same for cooling machinery. (Aittomäki and Aalto, 2012)

Outdoor heat pumps are a very common heat and cooling source in small residential buildings. The primary use of the heat pumps in residential buildings is for cooling and heating is only a side product. The pumps can be connected to either air or water circulation system. A special characteristic of outdoor heat pump is that its power output and coefficient of performance (COP) decrease when the temperature outside decreases. Thus, the outdoor heat pump may require additional heating system. Because the same heat pump can be used for both cooling and heating production, it provides a possibility to use the same machinery in producing heat and cooling simultaneously. (Aittomäki and Aalto, 2012, pp. 343-344) Figure 3.5 presents a configuration of a heat pump process. With a right process medium, it is possible to produce both cooling and heating simultaneously (Sarkar, Bhattacharyya and Gopal, 2006). With such a heat pump, cooling is produced at the evaporator and heating at the condenser.

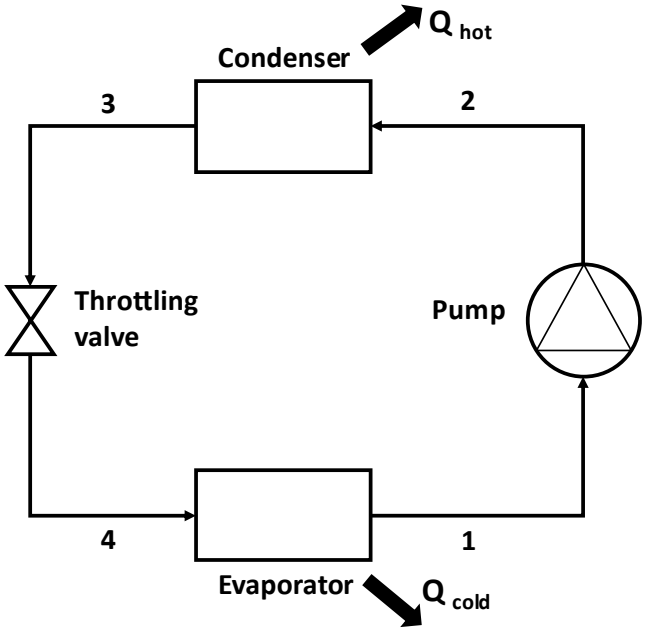

Figure 3.5 *A configuration of heat pump process. Based on* (Bellos and Tzivanidis, 2019)

COP is different for heating and cooling processes. For heating it is determined as

$$COP_{heating} = \frac{Q_{cond}}{W}, \tag{10}$$

where Q_{cond} is the heat removed from the system and W is the work of the compressor. For cooling COP is determined as

$$COP_{cooling} = \frac{Q_{evap}}{W}\ , \tag{11}$$

where Q_{evap} is the heat absorbed to the system. Q_{cond} is the energy that is released when the process medium condenses from vapor to liquid. Q_{evap} in turn is the energy needed to evaporate the liquid process medium back to vapor form. These can be calculated by

$$Q_{cond} = \dot{m}(h_4 - h_1), \tag{12}$$

$$Q_{evap} = \dot{m}(h_3 - h_2), \tag{13}$$

where $\dot{m}$ is mass flow rate through the condenser and evaporator, h is enthalpy for each point in Figure 3.5. The work used by the compressor is calculated in the same manner

$$W = \dot{m}(h_2 - h_1), \tag{14}$$

where $\dot{m}$ is the mass flow rate through the compressor and h is enthalpy for points before and after the compressor. (Bellos and Tzivanidis, 2019)

There is a wide range of refrigerants that can also be used in heat pumps. Each refrigerant is best suitable for different kind of applications depending on the temperature level. The most used refrigerants in heat pumps are R134a, R407C, R410A and propane. For heat recovery processes, where temperatures are higher, there are some special refrigerants, such as, R227ea and R236fa. (Aittomäki and Aalto, 2012, pp. 340) For heat pump systems, where the goal is to produce heating and cooling simultaneously, carbon dioxide is a potential refrigerant (Sarkar, Bhattacharyya and Gopal, 2006). Another heat pump application, in which CO_2 performs well, is domestic water heating. Temperature range of CO_2 goes as low as -54 °C. Higher temperatures, like 40–80 °C, are possible but also the pressure rises high (at 30 °C pressure is 72 bar). On the other hand, CO_2 has low viscosity, which means that pressure drops are small. The size of the compressor is small, since the energy gain per cubic metre is high due to big density of CO_2. And because the size of the heat exchangers is also smaller than with other refrigerants due to good heat transfer, the size of the whole system is smaller. (Aittomäki and Aalto, 2012, pp. 121-122)

3.6 Lithium ion battery

Li-ion batteries are quite new in the battery technology field. They could possibly revolutionize the renewable energy field by providing a possibility to store energy in major amounts. Li-ion batteries have a longer lifespan compared to other battery technologies. They also have higher power and energy densities. The problem, though, lies in the

costs, that are still too high. Renewables alone are not enough to boost the development of battery technology to make them more affordable. This would need the development of other possible applications, such as, electric cars and bikes and military and medical applications. At the moment one economically feasible MW-scale application for Li-ion battery systems is in controlling the power balance of power grids. (Diouf and Pode, 2015) Table 3.2 shows the characteristics of different kinds of batteries.

Table 3.2 *Comparison between different battery technologies. Modified from* (Diouf and Pode, 2015)

Specifications	*Lead acid*	*NiCd*	*NiMH*	*Li-ion*		
				Cobalt	Manganese	Phosphate
Spesific energy density [Wh/kg]	30–50	45–80	60–120	150–190	100–135	90–120
Cycle life (80 % discharge)	200–300	1000	300–500	500–1000	500–1000	1000–2000
Fast charge time [h]	8–16	1 typical	2–4	2–4	1 or less	1 or less
Maintenance requirement	3–6 months (topping charge)	30–60 days (discharge)	60–90 days (discharge)	Not required		
Safety requirements	Thermally stable	Thermally stable, fuse protection common		Protection circuit mandatory		
Toxicity	Very high	Very high	Low	Low		

As can be seen from Table 3.2, Li-ion batteries are superior on many aspects compared to other battery technologies. Li-ion batteries are low in toxics, they charge fast, are low

maintenance and have higher specific energy density. It must be pointed out though that the information is from 2015 and thus can be outdated.

Stationary application areas for Li-ion batteries can be divided into three: stand-alone systems or part of the electricity grid, size of the storage unit and the length of the discharge time. Discharge time is considered short, when it is less than one hour, and long when it is from one hour to several days. When the size of the battery is smaller than 100 kWh, it is a local storage system. For central storage systems the size of the battery is bigger than 1 MWh. Applications, such as uninterrupted power supply (UPS) and compensation of load peaks, work with local storage system and short discharge time. Although grid stabilization also works with short discharge time, it requires more energy and thus a central storage system. Central storage systems are also utilized with wind farms, arbitrage in the grid and central photovoltaic systems. (Korthauer, 2018) Arbitrage means the practice of purchasing electricity at a low price during low-demand-hours, storing it and discharging it with a higher price during the high-demand-hours (Zhang *et al.*, 2021). All of these require long discharge time, as well as, telecommunications, photovoltaic systems on buildings and arbitrage in the industrial sector. However, these applications utilize local storage systems. Li-ion batteries are great for short discharge time applications. (Korthauer, 2018) This is beneficial, especially with controlling the power balance of electrical grid, where fast response times are required. With long discharge time applications, Li-ion batteries compete with other battery technologies that are cheaper (Korthauer, 2018).

The application, the amount of energy to be stored and the discharge time define the technical requirements for energy storage batteries. Safety is prioritized, especially when the batteries are located inside buildings. The life span of these batteries can go up to 10 years, which can also mean high cycle numbers. Most applications do not require high energy density. Power density, in turn, is of great importance especially when it comes to applications with a short discharge time. Li-ion batteries have a high storage efficiency, which means that most of the stored energy can be released again. They can also store the energy for long periods without big power losses. This is called self-discharging. (Korthauer, 2018)

4. MATERIALS AND METHODS

This chapter presents the research strategy used in this thesis. It also presents the initial values that were used in the calculations, the actual calculations, and the basis for the economic feasibility analysis. It explains the choices behind some initial values and how the calculations were done. A more precise process chart of the systems is provided as well as a presentation of three cases according to which the calculations were run. Lastly it showcases the equations the economic feasibility analysis is based on.

4.1 Research strategy

The research methods in this study were a literature review, a process simulation, and an economic feasibility analysis. The study consists of four phases, which are presented in Figure 4.1. In the first phase of the research, trigeneration and its applications and possible technologies for trigeneration were studied through literature. The literature used consists of different research publications, basic literature of the energy technology field and statistics.

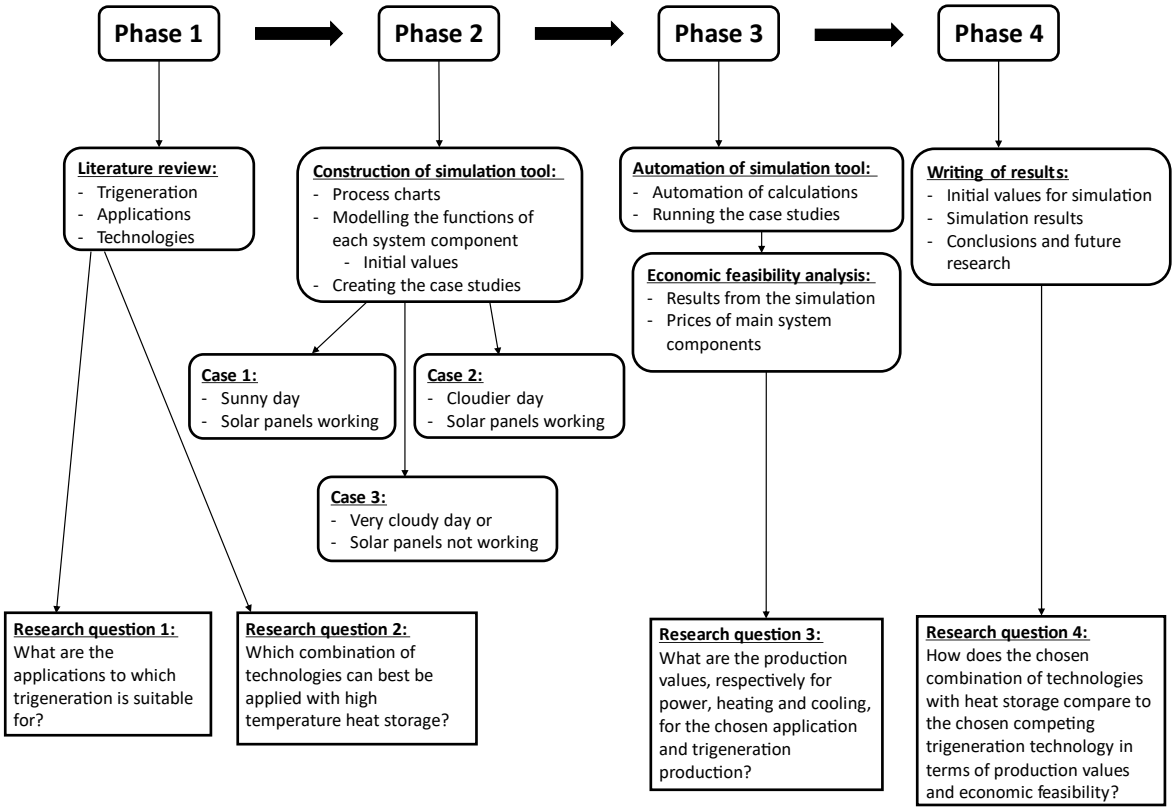

Figure 4.1 *Research process.*

The second phase consisted of constructing the process simulation tool and creating case studies that would test the systems in different ways. The first step in constructing the process simulation tool was to make process charts for both processes. The second step then was to model the functions of each system component through the process medium. This meant calculating the temperatures, pressures, mass flows, enthalpies, and entropies of the process mediums at different parts of the system. Initial values were determined along the calculations when needed. The third phase of the research started when the simulation tool could perform correct calculations on each process point manually. The first step was to make the calculations automated, so that the user could get the wanted results by only inserting a few initial values. The second step then was to run the different case studies on the now automated simulation tool. Lastly, with all the knowledge from the simulation, an economic feasibility analysis was performed.

The fourth and final phase of the research was to write down the initial values used in the simulation and the simulation results. The results were analysed, and some conclusions were made based on that. Ideas for future research were presented based on the whole research project.

4.2 Target application

The energy consumption numbers used in the calculations are based on a hospital in Finland. The hospital is in Raasepori and its area is 21590 m^2 (Hareja, 2021). The energy consumption numbers are based on (Hareja, 2021) and then were modified to fit the profile of a country with warmer climate (Bawaneh *et al.*, 2019). The electricity consumption used in the calculations was 5.48 MWh/d, the heat consumption was 4.11 MWh/d, and the cooling consumption was 1.37 MWh/d. The hourly profile of each energy form was created by hand taking into consideration the conditions of the application and the country. Since the application, where the calculations are applied to, is a hospital, the electricity consumption profile can thought to be quite level throughout the day. The hospital is also thought to be in a warm country, where the need for heating is rather small and the need for cooling significant. Naturally the need for cooling is greater during the day than during the night. Figure 4.2 presents the energy consumption profile for the target hospital, which was used in the calculations.

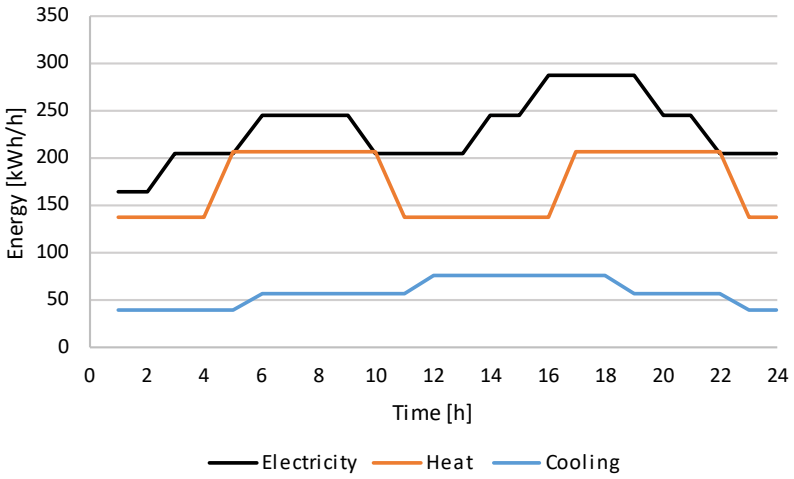

Figure 4.2 *Hourly energy consumption profile for a day for the target hospital.*

The energy supply values were provided by Polar Night Energy. The values are based on solar radiation energy values in Finland over a year. Figure 4.3 presents the energy supply profiles for the cases, which were used in the calculations. Two hourly profiles were chosen to represent different kind of weather conditions. A sunny day during the Summer (case 1 in Figure 4.3) was thought to be more representative of a normal day in a country with warmer climate than in Finland. The other hourly profile (case 2 in Figure 4.3) was chosen to represent a rather cloudy day.

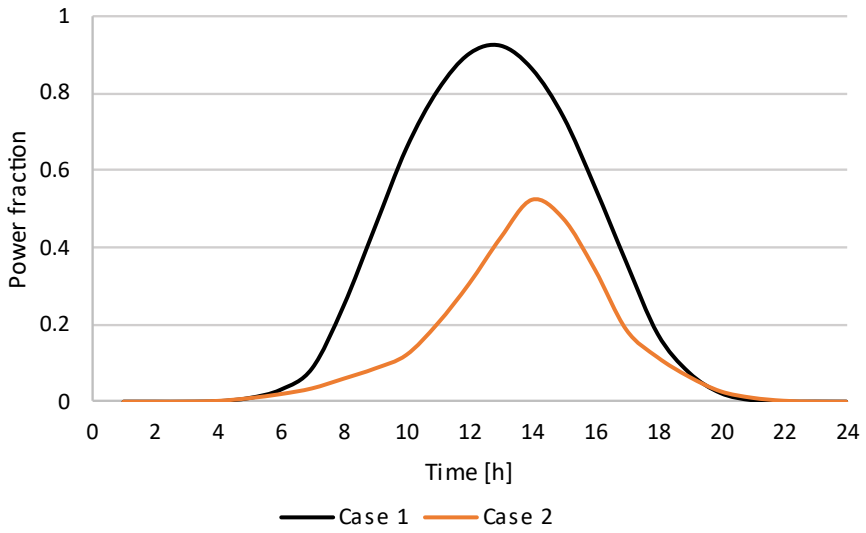

Figure 4.3 *Energy supply profiles for cases 1 and 2.*

As can be seen from Figure 4.3, the available energy differs a lot in these two cases. The solar panel power is a constant value of 2.7 MW meaning, that the solar panels were assumed to produce energy at power of 2.7 MW all the time. This power value was chosen as it is enough to raise the capacity of the heat storage back to its original value

when the storage is being loaded. These same profiles were used in the Li-ion battery calculations as well.

Different case situations were created for this study to thoroughly examine the functionality of these two systems.

CASE 1

The first case presents a situation, where there is solar energy available, but it is not enough to cover the energy demand for the whole day. It poses a rather normal situation since solar energy is not always available nor is it enough to cover the energy demand. This case provides information on the functionality of the system in normal circumstances.

CASE 2

The second case presents a similar situation as the first case in terms of operating the system. The difference between these two cases is in the available solar energy. In case 1, the total available solar energy is around 18.6 MWh while in case 2 the total available solar energy is 8.1 MWh. The two solar power profiles were presented earlier in Figure 4.3.

CASE 3

The third case presents a situation, where the energy storages in both systems have been loaded beforehand but not during the operation. It poses an extreme situation when there is no solar energy available. This case provides information on how long these systems can match the energy need of the end user.

4.3 Trigeneration production technology specifics

Two different trigeneration systems were studied in this thesis. Figure 4.4 presents simple system configurations for both systems. System 1 is a heat storage system and system 2 is a Li-ion battery system. They were studied as separate systems. Both, heat storage and Li-ion battery, are loaded with solar energy from the solar panels.

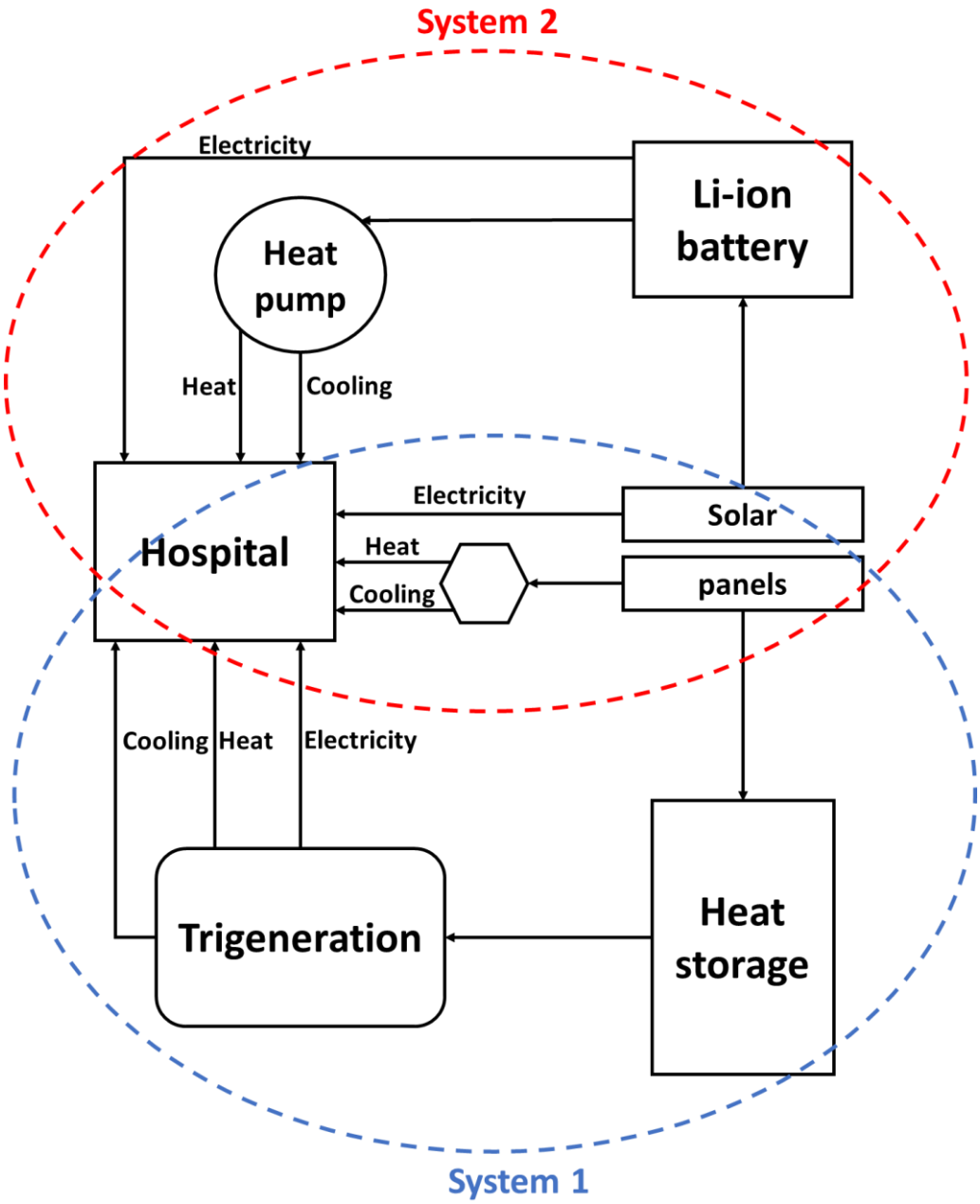

Figure 4.4 *System configurations for the studied processes.*

The main working principle for both systems is the same. When the solar energy from the solar panels is enough to cover the energy need of the target hospital, heat storage cycle nor the Li-ion battery cycle are not utilized. Electricity is then produced with the solar panels and heat and cooling with a heat pump or an absorption chiller or some other device. This has not been decided as it is not of interest in this study. However, when the solar energy is not enough to cover the demands of the hospital, heat storage cycle and Li-ion battery cycle are utilized to cover the demands. In system 1, heat from the heat storage is used in a trigeneration system to produce electricity, heat, and cooling

for the hospital. In system 2, electricity from the Li-ion battery is used to provide electricity for the hospital and run a heat pump, that produces heat and cooling.

Heat storage system

There were no official initial values for this studied process as the process has not been done in this way before. Some process values are based on the values provided by manufacturers, some on laws and regulations and some are purely educated guesses. The main process values that define the studied process are presented in Table 4.1.

Table 4.1 *Initial values for the heat storage system (Figure 4.5).*

Cycle	*Point*	*Temperature [°C]*	*Pressure [bar]*	*Volume flow [m^3/h]*
Heat storage	all		1*	
	A2b	270**		
	A3b	140**		
ORC	B1	320**	32*	
Absorption chiller	C1	80*	1**	60*
	C2	70*	1**	60*
	D1	7*	1**	91*
	D2	12*	1**	91*
	E1	35*	1**	212*
	E2	30*	1**	212*

* The value is based on the value provided by a manufacturer.

** The value is based on an educated guess.

The domestic water temperatures are regulated by law. The cold water temperature cannot overpass 20 °C (Ohje 2.3.6.1) and the hot water temperature must be between 55–65 °C (Määräys 2.3.8 and Määräys 2.3.9). (Ministry of Environment, 2007) The values chosen for this study are 10 °C for cold water and 60 °C for hot water.

The heat exchanger connecting A and B cycles (Figure 4.5) is thought to be three different heat exchangers: one heats up the toluene, one evaporates toluene and one superheats it. Because of the different application of each heat exchanger, they all have different overall heat transfer coefficients. The first and last heat exchangers are shell-and-tube heat exchangers while the middle one is naturally an evaporator. The first heat exchanger has liquid on one side and gas on the other side so its overall heat transfer

coefficient is 15–70 W/m^{2}K (*VDI Heat Atlas*. 2nd ed. 2010., 2010). For this study the chosen value was 70 W/m^{2}K. Toluene's circulation is produced by a pump, so the circulation is forced. The overall heat transfer coefficient for a forced circulation evaporator is 900–3,000 W/m^{2}K (*VDI Heat Atlas*. 2nd ed. 2010., 2010). The chosen value for this study was 900 W/m^{2}K. The last heat exchanger has gas on both sides of the shell-and-tube, so the overall heat transfer coefficient is 150–500 W/m^{2}K (*VDI Heat Atlas*. 2nd ed. 2010., 2010). For this study the chosen value was 400 W/m^{2}K.

Efficiency of the pump and isentropic efficiency of the turbine were needed for the ORC cycle calculations. The pump efficiency was chosen to be 80 % and the isentropic efficiency for the turbine was chosen to be 97 %. The molar masses of air and water were used in the energy balance equations (equation 9). The molar mass of air was 0.0289 kg/mol and the molar mass of water 0.018 kg/mol (Eronen *et al.*, 2019).

Li-ion battery system

The maximum capacity of the Li-ion battery is 3.2 MWh. The C-value of the battery is thought to be 1, which means that the maximum power for charging and discharging is 3.2 MW. ('A Guide to Understanding Battery Specifications', 2008). In the calculations the relation between energy and power is simple. If, for example, the required electric power is 30 kW, the capacity of the Li-ion battery decreases 30 kWh in one hour. The electrical power that is discharged from the battery consists of the power of the heat pump compressor and the overall electricity need of the hospital. The COP values for both heating and cooling are constant for the heat pump. A heat pump that produces heating and cooling simultaneously, has little higher values for COP than a heat pump that only produces heating or cooling. For this reason, the COP values chosen for these calculations are 4.5 for heating and 3.5 for cooling.

As the purpose of the heat pump is to produce domestic water heating, the HTF on the heating side is naturally water. The same regulations, decreed by the Finnish Ministry of Environment (2007), as for the heat storage system apply also for the Li-ion battery system. The temperature of the water therefore is 10 °C before entering the heat pump and 60 °C when the water exits the heat pump. On the cooling side, the HTF is air. As the hospital is thought to be located in a place with warm climate, the temperature of air before entering the heat pump is chosen to be 28 °C. Air temperature when exiting the heat pump is chosen to be 10 °C because public places are usually cooler in temperature than people's homes.

4.4 Simulation program

The process simulations for both systems were executed on Microsoft Excel. CoolProp for Excel was used with the heat storage system to access the thermodynamic values of toluene. CoolProp is a C++ library that implements eight different features. The most important features, considering this study, are pure and pseudo-pure fluid equations of state and transport properties for 122 components, mixture properties using high-accuracy Helmholtz energy formulations, and correlations of properties of incompressible fluids and brines. CoolProp supports for instance, in addition to Microsoft Excel, Python, Java and MATLAB. (*Welcome to CoolProp — CoolProp 6.4.1 documentation*, no date) After defining the initial values presented in chapter 4.3, rest of the process points were then calculated from basic thermodynamic formulas.

Heat storage system

The process is designed to work together with solar panels. The panels produce electricity that is used in heating resistors to heat up sand in the heat storage. The electricity produced by the panels is also used as it is and to generate heat and cold when the solar panel production is enough to cover the energy demand for the hour. When solar panels are enough to cover the energy demand, the heat storage system is not used. When the electricity production is not enough to cover the whole energy demand, it is used to only cover the electricity demand and heat and cold are produced with an absorption chiller or a heat pump. The heat storage system is utilized only when the solar panel production is not enough to cover any of the energy demands for the hour. Figure 4.5 presents the process chart for the studied heat storage process.

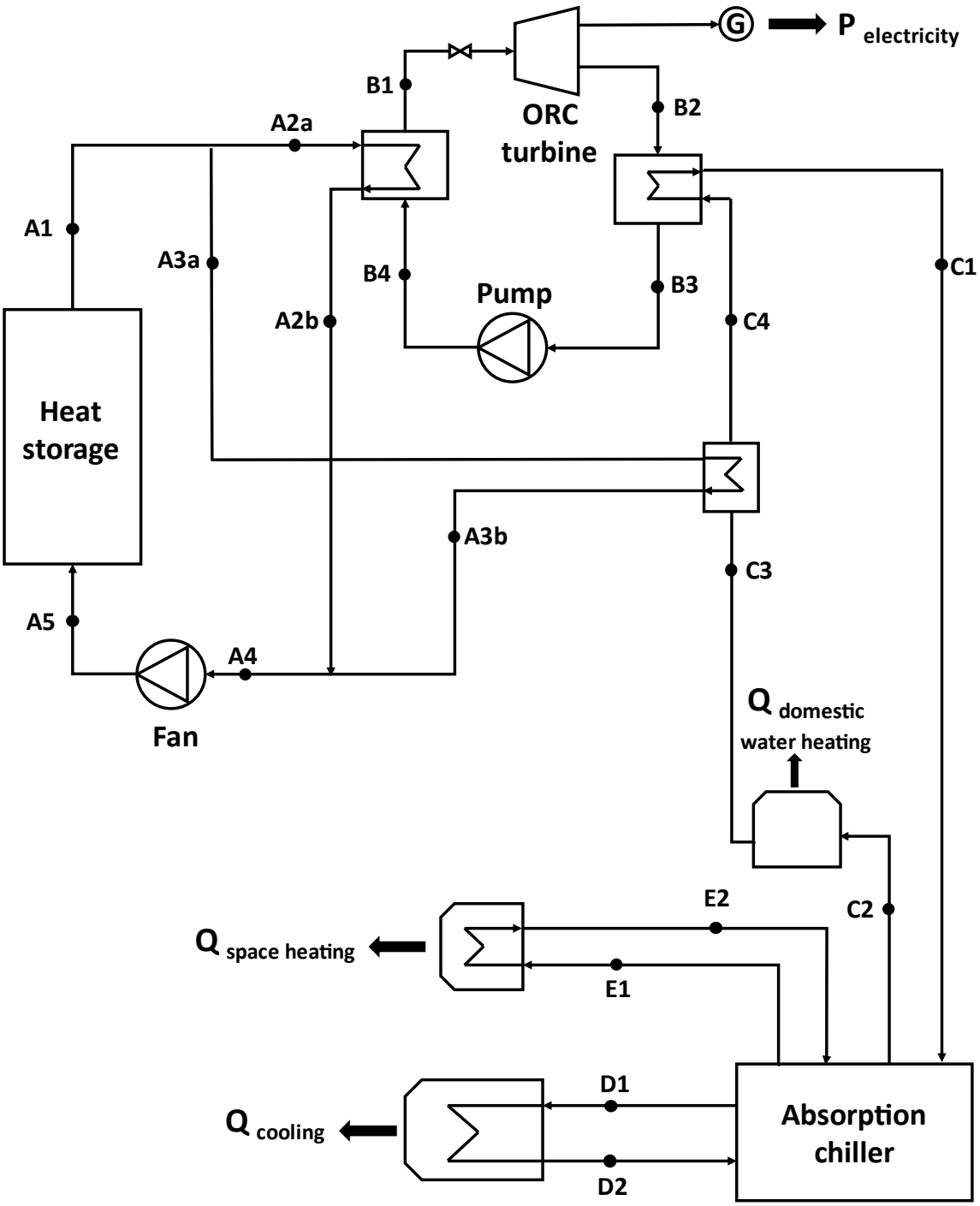

Figure 4.5 *Process chart of the heat storage system.*

The heat transfer medium in the heat storage cycle is air. The airflow at point A1 is divided into two different partial flows. One partial flow is used to heat up the process medium at points A3a and A3b and the other is used to evaporate process medium at points A2a and A2b. The mass flow in A3 partial flow is defined by using the heat exchanger balance formula (equation 9) and the mass flow in A2 partial flow is defined from the basic heat transfer equation. Thus, total air mass flow is the sum of these partial flows. The partial mass flows are combined and then led through a fan before entering

the heat storage. Because the flows were in different temperatures, mass flow at point A2b at 270 °C and mass flow at point A3b at 140 °C, a mass-fraction-based calculation was used in order to define the temperature of the combined flow.

The process medium in ORC-cycle is toluene. At point B1 super-heated toluene at the pressure of 32 bar and temperature of 320 °C enters a choke valve, whose purpose is to control the pressure and mass flow through the turbine to control the electricity generation. The mass flow of wanted electricity generation is calculated using equation 1. After the choke valve, toluene is led through the ORC-turbine, where toluene expands to its saturation pressure. The kinetic energy of the turbine is changed into electric energy by a generator connected to the turbine. After the turbine, toluene is in vapor form and is led to a condenser. Toluene first releases heat until it reaches the saturation temperature of 90 °C and then condenses into liquid and the heat released is transferred to the hot water cycle of the absorption chiller. The now saturated liquid toluene continues to a pump where its pressure is raised back to 32 bar. Lastly toluene enters a heat exchanger, where it is first heated up, then evaporated and finally superheated before it exits the heat exchanger.

The absorption chiller has three cycles. Each cycle produces a different product, depending on the temperature of the process medium. The process medium in all three cycles is water. Cycle C starts at point C1, where water enters the absorption chiller at the temperature of 80 °C. At point C2 water exits the absorption chiller at 70 °C and enters a heat exchanger. In the heat exchanger water releases heat, which is used to heat up domestic water supply for the application. This reduces the temperature to 68.2 °C (point C3) at which the water flow enters another heat exchanger, which is in charge of heating the water up to 80 °C, when ORC is not used. When ORC is in use, this heat exchanger is used to preheat the water flow to a temperature of 72 °C (point C4). After this, the water flow enters the condenser in B cycle. In the condenser, water is heated up to 80 °C. Cycle E is used to provide space heating for the application. Water enters a heat exchanger at 35 °C at point E1. After releasing heat, it exits the heat exchanger and enters the absorption chiller again at the temperature of 30 °C. Cycle D is similar to cycle E in terms of functionality. However, cycle D produces cooling instead of heating. Water flow at 7 °C enters a heat exchanger (point D1), where it receives heat, raising the temperature of the water flow to 12 °C (point D2).

The areas of the heat exchangers needed to be calculated for the economic feasibility analysis. With the three-stage heat exchanger between A and B cycles, the final temperatures of each stage were calculated using the basic heat transfer equation. All needed temperatures for the other heat exchanger were already known. To calculate the area of

each heat exchanger, a logarithmic mean temperature difference method (LMTD) was used. The temperatures at different stages of the heat exchangers were used to calculate the logarithmic mean temperature (equation 6) and then the logarithmic mean temperature with the overall heat transfer coefficients presented in the previous chapter were used in equation 7 to calculate the area of the heat exchanger.

The time span in the simulations was set to 24 hours. Each hour had its own energy demand and energy supply, which were tried to make meet. Energy demand consist of electricity, heat, and cooling consumption. Energy supply is the amount of electricity solar panels are able to produce. When the energy supply was not enough to cover the whole energy demand, second step was to compare the electricity consumption to the energy supply. If the energy supply was enough to cover the electricity consumption, ORC-turbine was not used, and heating and cooling were produced from different sources. All the energy demand that could not be covered with the energy from the solar panels was to be covered with the heat storage system. The heat storage system was run based on the electricity consumption. The amount of cooling, space heating and domestic water heating stays the same regardless of the electricity production from the ORC-turbine. When ORC-turbine is used, domestic water heating works as described earlier. However, when the ORC-turbine is not used, the temperature at points C4 and C1 becomes the same. Since the amount of energy needed for the heating of domestic water stays the same, the energy needed to heat up the water flow from the temperature of C4 to C1 becomes greater. This energy gap is covered by heat from the heat storage. Now for the hours, when the solar energy supply is enough and ORC-turbine is not used, the excess energy from the solar panels is used to load the heat storage.

Li-ion battery system

Just like the heat storage system, also the Li-ion battery system is designed to work together with solar panels. Figure 4.6 presents the process chart for the Li-ion battery system.

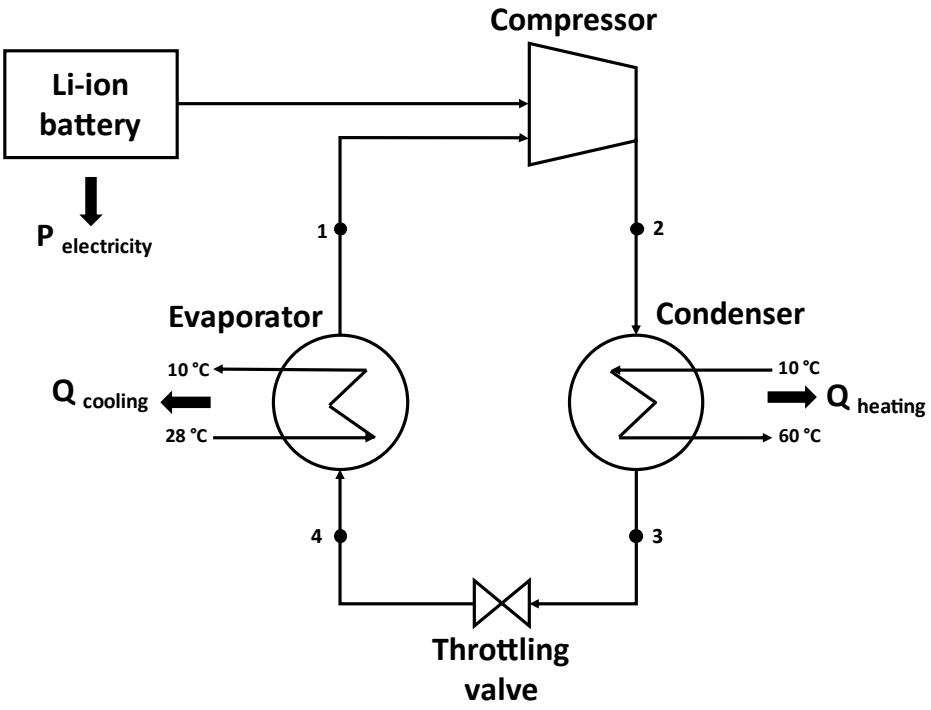

Figure 4.6 *Process chart of the Li-ion battery system.*

The process medium in the competing process is carbon dioxide. A compressor uses electricity from the Li-ion battery to compress the carbon dioxide flow to a higher pressure (point 1). After the compressor, carbon dioxide is led to a condenser (point 2), where it releases heat while going through a phase change. The now liquid carbon dioxide (point 3) expands in a throttling valve and continues to an evaporator (point 4). In the evaporator carbon dioxide goes through another phase change back to gas form by absorbing heat.

In the condenser, the HTF is water. Water goes in at the temperature of 10 °C. It heats up until 60 °C before exiting the condenser. Water is used for both space heating and as domestic water. The HTF in the evaporator is air. Air (at 28 °C) releases heat to carbon dioxide and thus its temperature decreases (to 10 °C) allowing cooling production. Electricity for the end user is taken straight from the Li-ion battery.

The energy demand and energy supply profiles are the same for the Li-ion battery system as for the heat storage system. The heating and cooling production of the system are calculated with equations 12 and 13. The mass flow rates for air and water in the evaporator and the condenser are calculated using iterations.

4.5 Economic feasibility

To get a better understanding of the economic situation, an economic feasibility analysis was done for both systems. The analysis examined capital expenses (CAPEX) and the life span of each system component. Both were estimated based on values found from different sources. The values used in the calculations are presented in Table 4.2.

Table 4.2 *Capital expenses and the life span of the system components.*

CAPEX	*Price [€]*	*Life span [years]*
Heat storage	1,000,000*	30*
ORC-turbine	820,533**	25*
Heat exchangers	159,768****	25*
Absorption chiller	62,000*	20*
Heat pump	40,000*	15*
Li-ion battery	1,446,400***	10*

* The value is based on information provided by Polar Night Energy.

** The value is based on information from (Arvay *et al.*, no date)

*** The value is based on information from (*Solar Off-Grid Lithium Battery Banks | BigBattery*, no date)

**** The value is based on information from (Capocelli *et al.*, 2020) and cost-to-capacity method.

Heat storage and Li-ion battery are both loaded with renewable energy and thus the energy itself is free of charge. Because of this OPEX are not included in the calculations. To simplify the calculations, only the main components in the system are included in CAPEX. “Heat exchangers” in Table 4.2 consists of all the different heat exchangers used in the heat storage system. The area of each heat exchanger was calculated using the LMTD method (equations 6 and 7) and then all the areas were summed together, and the price was calculated with cost-to-capacity method.

Annuity method is used to analyse the economic feasibility in a wider time frame. Annuity method is a method for calculating the depreciation on a fixed asset. Its purpose is to produce a constant annual charge for the total depreciation as well as produce a cost of an asset. (‘annuity method’, 2016) The adjusted annual costs of the system are determined as

$$P = A_{inv} + A_{oper} = c_{n/i} P_{inv,tot} + A_{oper} \quad (15)$$

where A_{inv} is the annual investment cost, A_{oper} is the annual operational costs, $P_{inv,tot}$ is the total investment cost of the system and $c_{n/i}$ is annuity factor. The annuity factor is calculated as follows

$$c_{n/i} = \frac{i(1+i)^n}{(1+i)^n - 1} \tag{16}$$

where n is the economic lifetime and i is imputed rate of interest. (Myllymaa, Holmberg and Ahtila, 2019) In this study, the imputed rate of interest i is 5 %. The economic lifetime of each component is presented in Table 4.2 as “Life span”.

Cost-to-capacity method is a tool used for cost estimations. It uses known costs and capacities to estimate the current costs of a piece of machinery or even of an entire facility. It is important to understand the characteristics of the facility, which is planned to be used in the project. (Richard K Ellsworth, 2009) Cost-to-capacity method is easy to apply for use and it gives a reasonable order-of-magnitude cost estimate quickly. Applications where great accuracy is required the cost-to-capacity method is not the best choice (REMER and CHAI, 1990) as it is classified as Class 5 or 4 by the Association for the Advancement of Cost Engineering (AACE). Class 5 is for the start of a project, when there is only limited information available, and Class 1 is for a fully defined project with many details. (*17R-97: Cost Estimate Classification System - AACE International*, no date) For optimal results, the technology of the facility, whose costs are being estimated, has to be the same or really close to the technology of the facility with known costs (*Cost-to-Capacity Method: Applications and Considerations - evcValuation*, no date).

Cost-to-capacity method can be defined as

$$\frac{C_2}{C_1} = \left(\frac{Q_2}{Q_1}\right)^x, \tag{17}$$

where C_1 is the known cost of facility 1, C_2 is the cost to be estimated for facility 2, Q_1 is the known capacity of facility 1, Q_2 is the known capacity of facility 2, and x is the scale factor for these two facilities (*Cost-to-Capacity Method: Applications and Considerations - evcValuation*, no date). This equation is used to calculate the costs of some of the technologies used in the simulations as no exact price was available for these process values.

5. RESULTS AND DISCUSSION

This chapter presents the simulation results for each case and for both combination of technologies. The results are analysed, and the main points are highlighted with figures. Comparison of technologies is performed considering the technical performance on each case and the economic feasibility of the systems. Lastly the possible aspects of future study are discussed shortly.

5.1 Heat storage system simulation results

The simulations were performed on three different case scenarios. The first case represented a normal day, when there is plenty of solar energy available. The second case represented a cloudier day, when the available solar energy is limited. The third case represented a day, when there is no solar energy available. The results for the heat storage system are presented in Table 5.1.

Table 5.1 *Heat storage system results.*

	ORC-turbine electricity generation [kW]		*Energy extracted from heat storage [kW]*		*Heat storage mean temperature [°C]*		*Heat storage outlet temperature [°C]*	
Day	max	min	max	min	max	min	max	min
Case 1	235	13	1,199	814	596	411	507	368
Case 2	218	13	1,174	815	515	359	446	329
Case 3	286	164	1,413	1,057	515	116	446	147

As can be seen from Table 5.1 case 1 has the highest temperatures for both the heat storage mean temperature as well as the outlet temperature. It also has the widest range in ORC-turbine electricity supply and the used energy from the heat storage. The less solar energy is available, the smaller the power range is with ORC electricity and heat storage energy and the lower the minimum temperatures are for the heat storage. Figure 5.1 shows how much and during which hours the solar panels can match the energy demand of the hospital in case 1. Between 7 and 18 o'clock the solar panels produce more energy than what is needed in the hospital. During these hours, the extra energy from the solar panels is used to load the heat storage. This results in higher temperatures in the heat storage, which can also be seen in Table 5.1.

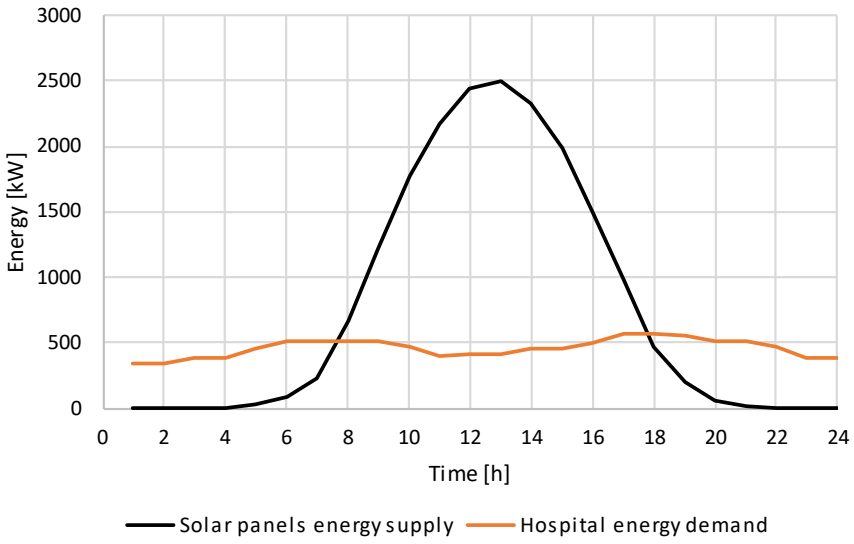

Figure 5.1. *Solar panels energy supply and hospital energy demand as a function of time in case 1.*

In case 2, the hours during which the solar energy produced is enough and ORC system is not used are narrowed. Figure 5.2 shows the relation between the energy supply and demand in case 2. As can be seen, the solar panels produce enough energy to cover the energy demand only between 11 and 17 o'clock. This is three hours less than in case 1 and can be seen in Table 5.1 in the lower heat storage temperatures and smaller energy range than with case 1.

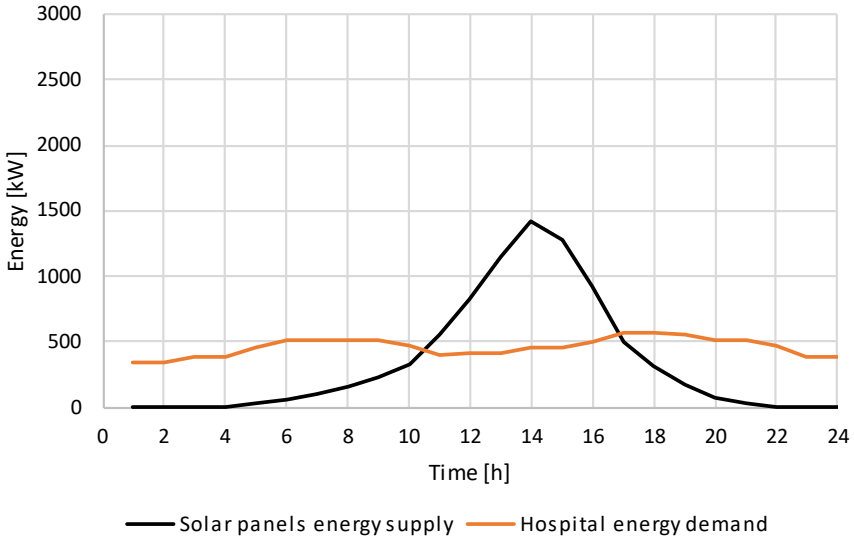

Figure 5.2. *Solar panels energy supply and hospital energy demand as a function of time in case 2.*

The heat storage capacity is 35 MWh at the beginning of the simulation. The heat storage is designed so that with the capacity of 35 MWh and solar panel power of 2.7 MW, the heat storage reaches its original capacity at the end of the day in case 1. Figure 5.3

shows two curves, which represent different variables in the heat storage simulation. The upper curve represents the variation in the capacity during the day in case 1. The curve below on the other hand represents the energy taken from or added to the heat storage at each hour of the day. As heat is taken from the heat storage, the amount of energy is negative and thus the capacity curve is a downward line. As stated before, between the hours of 8 and 18 o'clock, energy is added to the heat storage. This shows in Figure 5.3 as positive values in the energy curve and as a rising capacity curve.

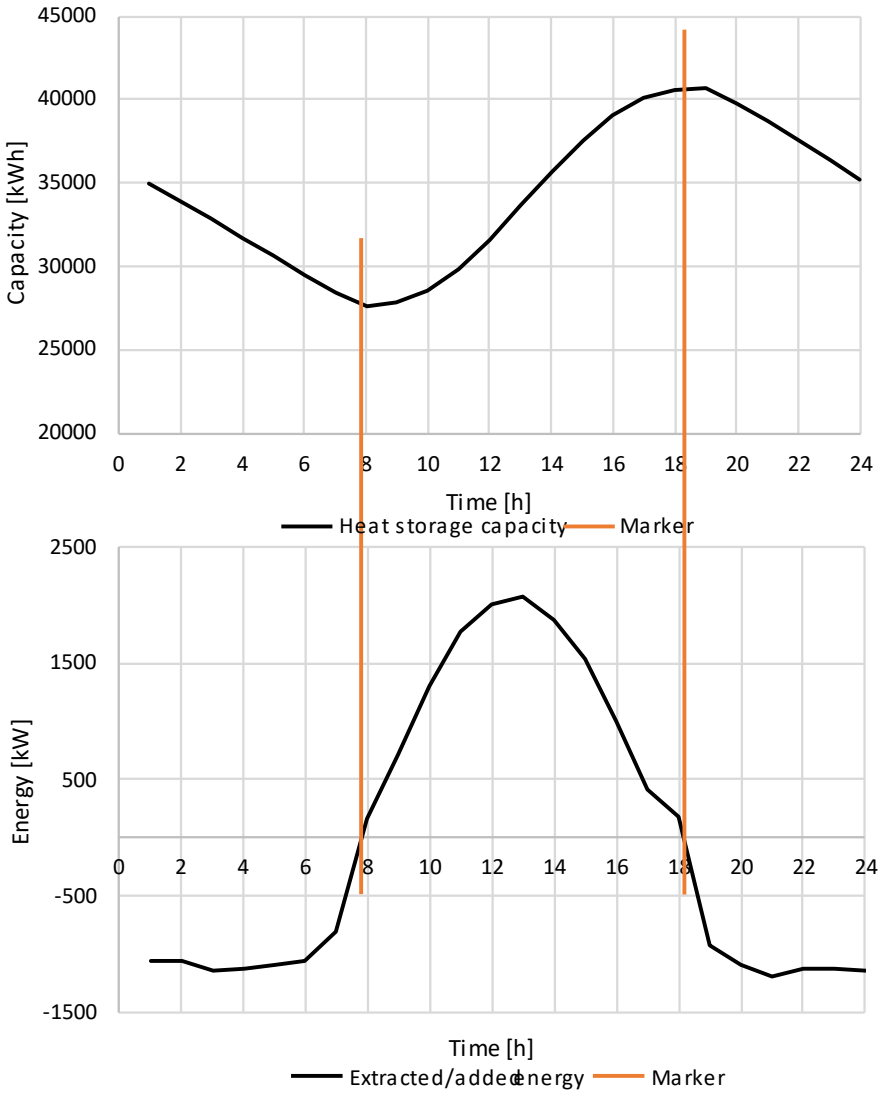

Figure 5.3. *The relation between heat storage capacity and heat storage energy in case 1.*

The ORC -turbine is utilized more in case 2 as the produced solar energy is less than with case 1. This same effect can be seen in Figure 5.4, where the upper curve represents the variation in capacity during the day and the lower curve represents the energy taken from or added to the heat storage. Unlike in case 1, the capacity does not reach its original value of 35 MWh at the end of the day. This is due to both smaller amount of

energy added to the heat storage and longer period of time, when energy is taken from the heat storage. The shape of the curves is similar to the curves in Figure 5.3, though between 10 and 18 o'clock the capacity curve does not rise as strongly due to the reasons explained earlier.

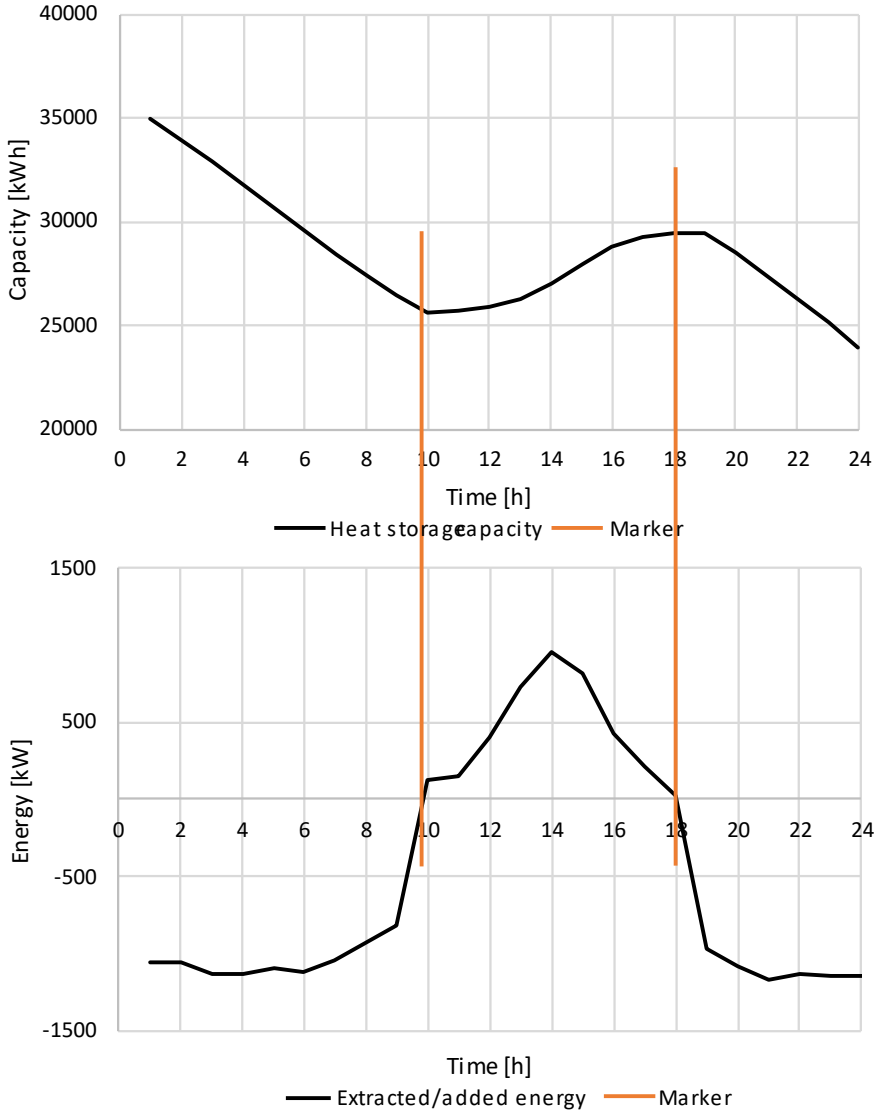

Figure 5.4. *The relation between heat storage capacity and heat storage energy in case 2.*

For case 3 the situation is different in many ways. The heat storage has been loaded to the capacity of 35 MWh beforehand and is not loaded during the day. Thus, it is not reasonable to present the curves for heat storage capacity and energy, as they all follow the form of the outlet temperature curve in Figure 5.5. The outlet temperature of the heat storage decreases gradually as more heat is taken from the heat storage, but none is added to it. If all the energy could be drained from the heat storage, it would eventually reach the temperature of 0 °C. However, this is not possible, as for the ORC-cycle to

work properly, the temperature of toluene, before it enters the turbine, must be 320 °C. Thus, the lowest outlet temperature, in which the heat storage system works, is 340 °C. To ensure that the system operates smoothly, the lowest outlet temperature is set to 360 °C (orange line and dot in Figure 5.5) and the lowest mean temperature of the heat storage is 400 °C. As can be seen from the figure, the lowest possible operating point is reached in around eight hours in case 3. This means that the heat storage system is able to cover the energy demand of the hospital only for the first eight hours. After this point, the energy demand must be covered in other ways.

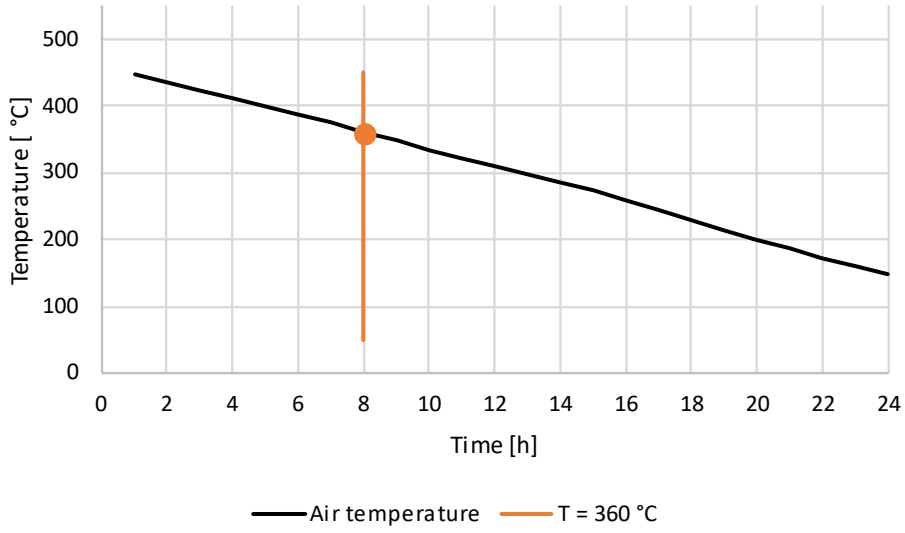

Figure 5.5. *Outlet temperature of the heat storage in case 3.*

This same issue occurs with case 2. Because the energy added to the heat storage during the peak solar hours is not enough to raise the capacity back to its original level, the outlet temperature also remains lower. The orange line and dot in Figure 5.6 represent the moment when the outlet temperature is at 360 °C. This happens after around 21 hours. Similarly, to case 3, during the last three hours of the day, the energy demand of the hospital must be covered with some other energy source, as the heat storage system is not able to cover the whole day with these initial values for case 2.

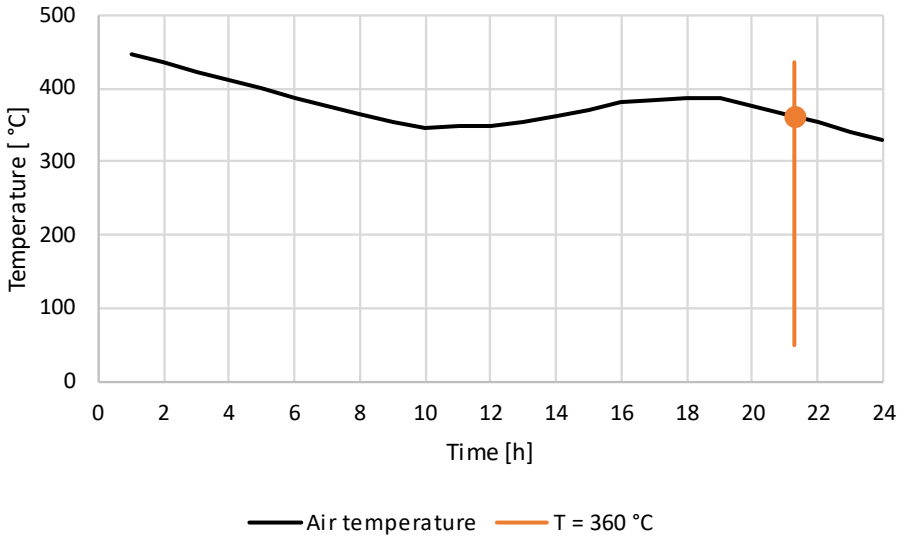

Figure 5.6 *Outlet temperature of the heat storage in case 2.*

The final production values are the same for all three cases in case of cooling and heating. Heating is divided into space heating and domestic water heating as they are produced at different parts of the process. The production value for cooling is 530 kW, for space heating 1,223 kW and for domestic water heating 119 kW. As the use of ORC-cycle does not define the process values for these products, the production of cooling and heating stays the same throughout the day.

5.2 Li-ion battery system simulation results

The same three cases were driven for the Li-ion battery system. Just like with the heat storage system, the Li-ion battery was designed so that with the capacity of 2 MWh and solar panel power of 2.7 MW, the capacity of the battery would return to 2 MWh at the end of the day. Because the Li-ion battery process is driven based on the heat demand (Figure 4.2), the process values stay the same in all three cases. The difference between the three cases is in the variation of these process values as they are not always the same at the same hour. Table 5.2 presents the process values for the Li-ion battery system.

Table 5.2 *Process values for Li-ion battery system.*

	max	*min*
Heating [kW]	205.5	137.0
Cooling [kW]	159.8	106.5
Compressor power [kW]	45.6	30.4
Total electricity removal from Li-ion battery [kW]	331.9	194.0

Figure 5.7 shows how the total electricity removal from the battery is divided between the electricity demand of the compressor of the heat pump and the electricity demand of the hospital and how the capacity of the Li-ion battery varies during the day in case 1. As can be seen from the figure, when electricity is taken from the battery, its capacity decreases. Between 8 and 18 o'clock, the battery is charged with excessive solar energy until it reaches its maximum capacity which is 3,2 MWh. This retells the energy supply and demand curves in Figure 5.1 as expected.

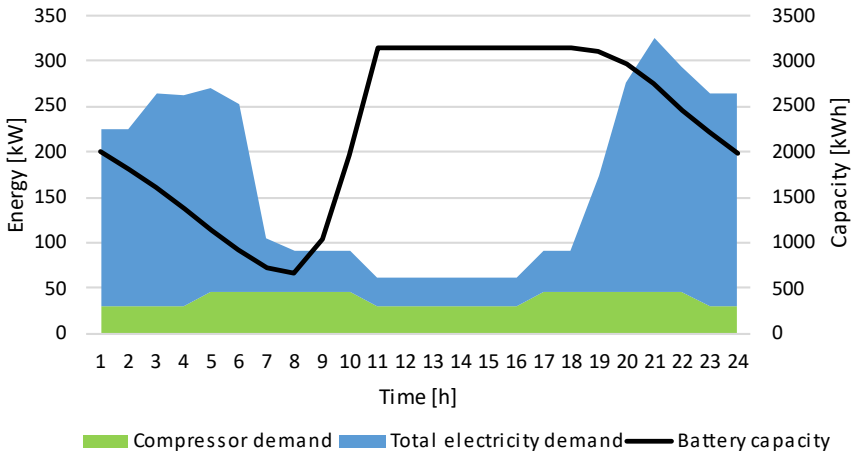

Figure 5.7 *The relation between Li-ion battery capacity and electricity removal from the battery in case 1.*

In case 2, compressor power and the total electricity demand stay the same in comparison to case 1 but since energy supply from the solar panels is less, more is required from the Li-ion battery. Figure 5.8 presents the relation between Li-ion battery capacity and electricity removal from the battery in case 2. The difference between case 1 and case 2 is that in case 2, the solar panels produce enough energy to start charging the Li-ion battery at around 10 o'clock while in case 1 this happened at 8. This also results in the capacity of the battery to reach smaller values: the minimum capacity value of the Li-

ion battery is around 300 kWh in case 2 while in case 1 the minimum value is around 650 kWh. Naturally the maximum capacity value is also reached later, at around 14 o'clock, in case 2.

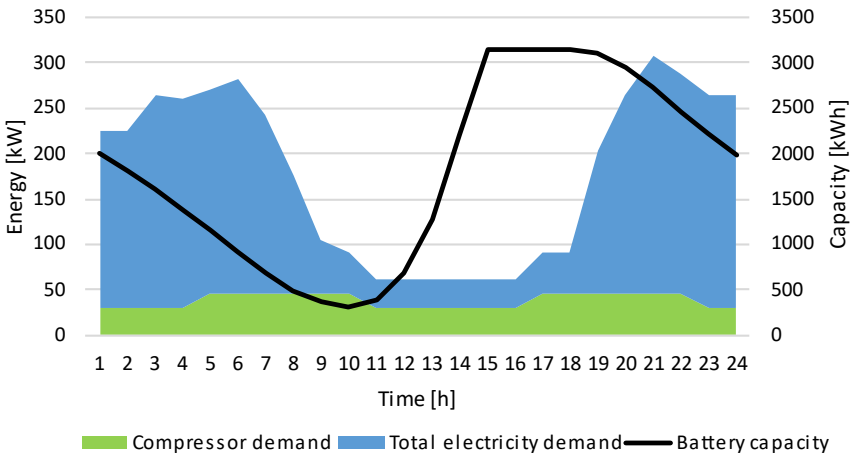

Figure 5.8 *The relation between Li-ion battery capacity and electricity removal from the batter in case 2.*

Case 3 is a bit different since there is no solar energy available at any point of the day and therefore the Li-ion battery is not charged. This can be seen in Figure 5.9, which shows how the capacity of the Li-ion battery decreases during the day and also how the need for electricity varies throughout the day. On a day with no solar energy available or with the solar panels on a service break, the hospital would need to use external energy for 15 hours a day. For the Li-ion battery to be enough for the whole day, the capacity of the battery would have to be 6.2 MWh.

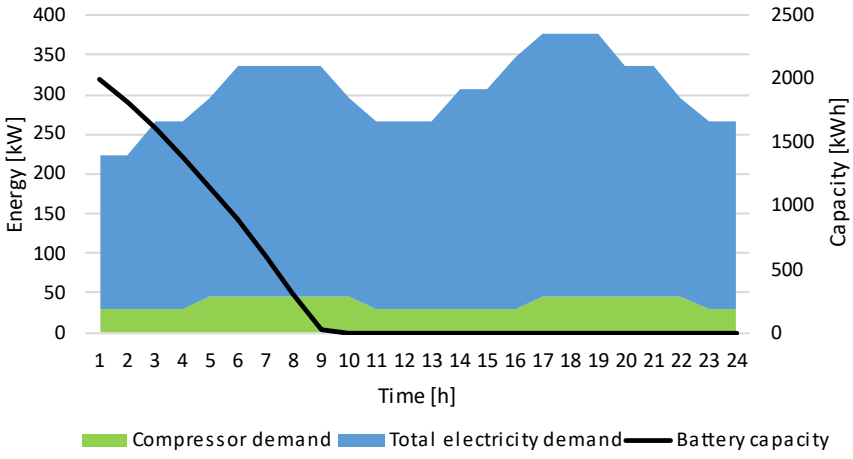

Figure 5.9 *The relation between Li-ion battery capacity and electricity removal from the battery in case 3.*

5.3 Results of economic feasibility analysis

Another thing that was calculated during this process, was the price of both of the systems. Each system was broken down to its main components, which were heat storage, ORC, heat exchangers and absorption chiller in the heat storage system and Li-ion battery and heat pump in the Li-ion battery system. The prices and life spans of each component were presented in Table 4.2. The annuity method was used to calculate the annual costs of each component and the results are presented in Table 5.3.

Table 5.3 *Annual costs of the systems and their main components.*

Component	*Heat storage system [€/a]*	*Li-ion battery system [€/a]*
Heat storage	65,051.44	
ORC-turbine	58,218.83	
Heat exchangers	11,335.97	
Absorption chiller	4,975.04	
Li-ion battery		187,315.42
Heat pump		3,853.69
Total annual costs	139,581.28	191,169.11

As can be seen from Table 5.3 Li-ion battery is the most expensive component while heat pump is the cheapest one. All the components in the heat storage system fall in between these prices. Cost-to-capacity method (equation 17) was used to calculate the price of the heat exchangers. Other prices were based on different sources presented in chapter 4.5. The total annual costs for both systems exceeded 100,000 euros and the Li-ion battery system almost reached 200,000 euros. If the hospital were to buy all the energy it needs, the annual price would be around 280,000 euros. This price is based on the energy consumption profile (Figure 4.2) and market energy prices in Finland. With these prices, it would be profitable for the hospital to utilize either of the systems instead of buying the energy from the market. Obviously, this is a very rough analysis on the economic feasibility of these systems as well as the option to buy from the market and no further decisions should be made according to this.

5.4 Analysis of chosen technologies

The simulation results for the heat storage system and the Li-ion battery system were presented in the previous chapters. The results include the process values, figures, and analysis on how well each system can match the energy demand of the hospital and the total annual costs of the systems. The results were presented separately for both systems and the aim of this chapter is to compare these results to each other.

The process values for both processes matched the demand and, in some cases, also exceeded them. This was due to the design point of view as both systems were simulated so that the limiting factor (electricity for the heat storage system and heat for the Li-ion battery system) was always met. Thus, the other process values exceeded their demands. The heat storage system produced almost seven times more cooling than what the maximum need was. With Li-ion battery system this number was approximately 1.4. The combined heat production from the heat storage system was 1,342 kW, which is 6.5 times more than the maximum heat demand while Li-ion battery system produced exactly the heat demand as it was the limiting factor for that system. Electricity production for both systems matched the demand, since electricity was the limiting factor for the heat storage system and Li-ion battery is an energy storage whose output energy form is electricity.

In cases 1 and 2, there is more solar energy available than what the total demand is. This results in extra solar energy during some hours of the day and that energy is used to charge and load the storages. With the heat storage system, the extra solar energy is transformed into heat. The heat storage can receive heat until the mean temperature of the heat storage is around 600 °C. As can be seen from Table 5.1 the maximum heat storage mean temperature is 595 °C, which means that the heat storage can receive all the extra solar energy the solar panels produce. The operating principle of the Li-ion battery is different. It cannot receive all the extra solar energy if the battery is already full and thus the leftover solar energy goes to waste.

The total annual prices as well as the annual prices for the main components were presented earlier in Table 5.3. The price difference in the total annual prices between the heat storage system and the Li-ion battery system is notable, around 50,000 euros for the benefit of the heat storage system. The Li-ion battery is the most expensive component of all the components listed exceeding the price of the heat storage with about 120,000 euros. The components in the heat storage system are more on the same price range, except for the absorption chiller, which is clearly cheaper than the rest of the components.

One of the biggest differences between the heat storage and the Li-ion battery is their size in terms of capacity. The capacity of the heat storage is around 17 times greater than the capacity of the Li-ion battery. This is most likely an efficiency question. The electricity produced by the solar panels is transformed into heat in the heat storage and then later again transformed into electricity by the ORC generator. The electricity transformed into heat is also used as heat in the process to produce heat and cooling. The energy running in the process changes form twice, which increases the energy losses. Another reason for the bigger capacity, is the need of heat, which is bigger than the need of electricity, to produce the desired amount of energy. To produce 338 kWh of energy in the form of electricity, heat and cooling, the heat storage system requires 1,057 kW of heat while the Li-ion battery requires 194 kW of electricity, which consists of the electricity demand of the hospital and the power demand of the heat pump. The Li-ion battery system is also more straightforward as the electricity from the solar panels is stored as electricity and then later it is transformed into heat and cooling in the heat pump. Thus, the Li-ion battery is more efficient, because it can produce the desired amount of energy with smaller capacity.

5.5 Future work

In the future, were this research to continued, there are a few issues to focus on. The first one is the execution of cooling, when the process runs solely on solar power. This kind of situation would happen daily during the sunny hours of the day and the heat storage system would be utilized at night, when there is no sunlight available. There are three different possibilities to solve the cooling problem. First one is a cooling compressor that takes the needed power straight from the solar panels. Second option is to use the absorption chiller from the heat storage system and power it also with the solar panels. The downside of this, though, is its small COP, which results in rather bad efficiency. To tackle the low-efficiency-issue, a second heat storage could be added to the system. Cooling would be produced with the absorption chiller but instead of using the cool right away, it is stored in a water storage. The problem to solve in the future is which of these three options has the best efficiency-cost-effectiveness-rate.

Another thing to focus on are the weather conditions. Weather conditions vary significantly in different locations and also throughout the year. There are important questions that need to be answered when determining whether this combination of technologies is best suitable for the conditions at the location of interest. How much does the weather affect the production? Is the production still profitable in these weather conditions? Is the

system able to produce enough energy to meet the needs of the application throughout the year?

With the world slowly trying to shift to more environmentally friendly energy production options and manufacturing in general, it is only natural to dig deeper into the emissions and other environmental effects these two systems might have. Batteries contain metals that are rare, expensive and their mining has severe environmental and social effects (Castelvecchi, 2021). Surely this is a problem on its own, but it becomes an even greater problem as the world is transitioning away from fossil fuels to renewable energy and electric vehicles, which rely heavily on batteries, should we desire to keep this standard of living we now have. According to Castelvecchi (2021) a Li-ion battery pack for electric vehicle could contain 8 kg of lithium, 35 kg of nickel, 20 kg of manganese and 14 kg of cobalt. The capacity of electric vehicles batteries varies between 17.6 kWh–100 kWh (*Electric-Vehicle Battery Basics*, no date). The capacity of the Li-ion battery in this study was 3.2 MWh which is 32 times more than the maximum capacity of an electric vehicle battery. The amount of materials needed for a battery of this size must also exceed the amounts mentioned in (Castelvecchi, 2021) in multiples thus increasing the environmental and social effects as well. Whether it is actually environmentally sensible to utilize such a system is a topic for future research. The environmental effects of manufacturing the heat storage system on the other hand, are unknown and have not been studied before. The heat storage itself can reduce CO_2 emissions by several tons a year (Mission Innovation, 2020) but the question for future research is, whether the manufacturing of the heat storage system has environmental effects or not, and what those effects are.

While the results show that the price of the heat storage system is lower than the price of the Li-ion battery system, the components of these system differ in the age of the technology. Li-ion batteries and heat pumps are older, well-known, and well-developed technologies while absorption chiller and ORC are newer and not so widely used. The development of Li-ion batteries is fast, and the prices have come down fast in past years. What is the situation for absorption chillers and ORC? There is space to study these technologies and the processes they are utilized in. Are there possibilities to develop these technologies? What happens to the prices in the future? What about efficiencies? Could it be, that, in the future, the Li-ion battery system becomes cheaper than the heat storage system? These are all valid question that can be answered should this work be continued in the years to come.

6. CONCLUSIONS

The purpose of this thesis was to study trigeneration with a heat storage system and compare it to a Li-ion battery system. The research questions covered the possible applications for trigeneration as well as the suitable technologies that could be combined with the heat storage in order to enable trigeneration production with it. Other research questions covered the process and production values and the comparison of the two systems. The research methods used to conclude this study were literature review, a process simulation, and an economic feasibility analysis.

Trigeneration is a means of energy production where electricity, heat and cooling are all produced simultaneously. A requirement for a feasible trigeneration system is that all three energy forms are needed throughout the year. On the other hand, trigeneration also has great advantages over traditional power plants or CHP systems. Trigeneration has, for instance, an ability to run on multiple fuels, lower fuel consumption and higher overall efficiencies. Possible applications for a trigeneration system are hospitals, hotels, office buildings and schools or universities.

The heat storage system in this study consists of a heat storage, ORC-turbine, absorption chiller and different types of heat exchangers. The heat storage is loaded with energy from solar panels and then the heat from the storage is used in different parts of the system to produce electricity, heat, and cooling. Electricity is produced with the ORC-turbine, whose process medium is toluene. Absorption chiller is responsible for producing both heat and cooling and it is connected to the ORC-cycle with a heat exchanger. The process medium in the absorption chiller is water and in the heat storage cycle it is air. The Li-ion battery system consists of two components: a Li-ion battery and a heat pump. The heat pump uses electricity from the battery to produce heat and cooling at the same time. The process medium in the heat pump is CO_2 and the HTFs are water on the heating side and air on the cooling side.

A process simulation was done to both systems. The application chosen for the simulation was a hospital in Finland, whose energy consumption profile was modified to better fit the consumption profile in country with warmer climate. The energy consumption profile was an hourly profile, and it was done for 24 hours. The initial values for the simulations were gathered from different sources and some were based on laws and regulations or on educated guesses. There were three different case studies that were run for

both systems. The first case represented a normal sunny day, the second case represented a cloudier day, and the third case represented a day with either no sunlight available or the solar panels on a service break. The same energy consumption values were used for all three cases. In addition to the production values an economic feasibility analysis was performed on both systems to determine which of the systems had smaller investment costs.

The results showed that both systems were able to meet the energy demands of a hospital in cases 1 and 2 and failed to meet those demands in case 3. The heat storage system produced excess cooling and heating as it was run based on the electricity demand. During the hours when the solar panels produced more energy than needed, the excess energy was used to load the heat storage. Because the maximum mean temperature of the heat storage in the simulations was below the maximum temperature of the heat storage structures, the heat storage could receive all the excess energy from the solar panels. The Li-ion battery system produced only excess cooling as it was run based on the heat demand and because it is an energy storage for electricity. However, the Li-ion battery system is not spared from waste energy, as it cannot receive all the extra energy the solar panels produce during peak solar hours. Since the systems performed as well in terms of meeting the energy demands, differentiating them came down to the investment costs. The annual costs of the Li-ion battery system were significantly bigger than the annual costs of the heat storage system. The annual costs the Li-ion battery were the biggest of all the components in both systems and the cost of the heat pump were the smallest. The annual costs of the heat storage components fall in between these two, the costs of the heat storage being the biggest.

Considering the costs of these systems, the heat storage system is a more sensible choice for industrial scale applications. However, it is a more complex system and requires more space and maintenance. In the future, possible research subjects include technology and price development of both systems, environmental effects of manufacturing these technologies, solutions to the problem of having no sunlight available and the effects of different seasons and weather conditions.

REFERENCES

17R-97: Cost Estimate Classification System - AACE International (no date). Available at: https://www.yumpu.com/en/document/read/28534733/17r-97-cost-estimate-classification-system-aace-international (Accessed: 18 May 2022).

'A Guide to Understanding Battery Specifications' (2008).

Aittomäki, A. and Aalto, E. (2012) 'Kylmätekniikka'. Edited by A. Aittomäki and E. Aalto. Helsinki: Suomen kylmäyhdistys.

Al-Sulaiman, F. A., Dincer, I. and Hamdullahpur, F. (2013) 'Thermoeconomic optimization of three trigeneration systems using organic Rankine cycles: Part I – Formulations', *Energy Conversion and Management*, 69, pp. 199–208. doi: https://doi-org.libproxy.tuni.fi/10.1016/j.enconman.2012.12.030.

Al-Sulaiman, F., Dincer, I. and Hamdullahpur, F. (2013) 'Thermoeconomic optimization of three trigeneration systems using organic Rankine cycles: Part II – Applications', *Energy conversion and management*, 69, pp. 209–216. doi: 10.1016/j.enconman.2012.12.032.

Alva, G., Lin, Y. and Fang, G. (2018) 'An overview of thermal energy storage systems', *Energy (Oxford)*, 144, pp. 341–378. doi: 10.1016/j.energy.2017.12.037.

'annuity method' (2016) *A Dictionary of Accounting*. 5th edn. Oxford University Press.

Arvay, P. *et al.* (no date) 'Economic Implementation of the Organic Rankine Cycle in Industry'.

Bawaneh, K. *et al.* (2019) 'Energy Consumption Analysis and Characterization of Healthcare Facilities in the United States', *Energies (Basel)*, 12(19), p. 3775. doi: 10.3390/en12193775.

Bellos, E. and Tzivanidis, C. (2018a) 'Investigation of a hybrid ORC driven by waste heat and solar energy', *Energy conversion and management*, 156, pp. 427–439. doi: 10.1016/j.enconman.2017.11.058.

Bellos, E. and Tzivanidis, C. (2018b) 'Multi-objective optimization of a solar driven trigeneration system', *Energy*, 149, pp. 47–62. doi: https://doi-org.libproxy.tuni.fi/10.1016/j.energy.2018.02.054.

Bellos, E. and Tzivanidis, C. (2019) 'A comparative study of CO2 refrigeration systems', *Energy Conversion and Management: X*, 1, p. 100002. doi: 10.1016/J.ECMX.2018.100002.

Bianco, V. *et al.* (2017) 'Modeling energy consumption and efficiency measures in the Italian hotel sector', *Energy and Buildings*, 149, pp. 329–338. doi: 10.1016/J.ENBUILD.2017.05.077.

Buonomano, A. *et al.* (2015) 'Energy and economic analysis of geothermal–solar trigeneration systems: A case study for a hotel building in Ischia', *Applied Energy*, 138, pp. 224–241. doi: https://doi-org.libproxy.tuni.fi/10.1016/j.apenergy.2014.10.076.

Capocelli, M. *et al.* (2020) ‘Reuse of Waste Geothermal Brine: Process, Thermodynamic and Economic Analysis’, *Water (Basel)*, 12(2), p. 316. doi: 10.3390/w12020316.

Castelvecchi, D. (2021) ‘Electric cars and batteries: how will the world produce enough?’, *Nature 2021 596:7872*. Available at: https://www.nature.com/articles/d41586-021-02222-1 (Accessed: 23 May 2022).

Chen, J. M. P. and Ni, M. (2014) ‘Economic analysis of a solid oxide fuel cell cogeneration/trigeneration system for hotels in Hong Kong’, *Energy and Buildings*, 75, pp. 160–169. doi: https://doi-org.libproxy.tuni.fi/10.1016/j.enbuild.2014.01.053.

Cost-to-Capacity Method: Applications and Considerations - evcValuation (no date). Available at: https://evcvaluation.com/cost-to-capacity-method-applications-and-considerations/ (Accessed: 28 March 2022).

Cotana, F. *et al.* (2014) ‘Comparison of ORC Turbine and Stirling Engine to Produce Electricity from Gasified Poultry Waste’, *Sustainability*, 6(9), pp. 5714–5729. doi: http://dx.doi.org/10.3390/su6095714.

Dinçer, I. and Rosen, M. (Marc A.) (2010) *Thermal energy storage systems and applications*. 2nd edn. Hoboken, N.J: Wiley.

Diouf, B. and Pode, R. (2015) ‘Potential of lithium-ion batteries in renewable energy’, *Renewable Energy*, 76, pp. 375–380. doi: 10.1016/J.RENENE.2014.11.058.

Electric-Vehicle Battery Basics (no date). Available at: https://www.myev.com/research/ev-101/electric-vehicle-battery-basics (Accessed: 23 May 2022).

Eronen, J. *et al.* (2019) *MAOL-taulukot*. 1. painos. Edited by J. Eronen et al. Helsingissä: Kustannusosakeyhtiö Otava.

Fong, K. F. and Lee, C. K. (2017) ‘Investigation of climatic effect on energy performance of trigeneration in building application’, *Applied Thermal Engineering*, 127, pp. 409–420. doi: https://doi-org.libproxy.tuni.fi/10.1016/j.applthermaleng.2017.08.049.

Fuls, W. F. (2017) ‘Enhancement to the Traditional Ellipse Law for More Accurate Modeling of a Turbine With a Finite Number of Stages’, *Journal of engineering for gas turbines and power*, 139(11). doi: 10.1115/1.4037097.

Hareja, O. (2021) ‘SAIRAALOIDEN ENERGIA-ANALYYSI JA MAHDOLLI-SUUDET HIILINEUTRAALIIN ENERGIANKULUTUKSEEN Hospitals’ energy analysis and opportunities for net zero carbon energy consumption’.

Hewitt, G. F. (ed.) (1990) ‘Hemisphere handbook of heat exchanger design’. New York, NY: Hemisphere.

IEA – International Energy Agency (no date). Available at: https://www.iea.org/ (Accessed: 22 December 2021).

Jafary, S. *et al.* (2021) ‘A complete energetic and exergetic analysis of a solar powered trigeneration system with two novel organic Rankine cycle (ORC) configurations’, *Journal of cleaner production*, 281. doi: 10.1016/j.jclepro.2020.124552.

Jiang, J. *et al.* (2016) ‘Performance Analysis of CCHP System for University Campus

in North China', *Procedia, social and behavioral sciences*, 216, pp. 361–372. doi: 10.1016/j.sbspro.2015.12.049.

Korthauer, R. (2018) *Lithium-Ion Batteries: Basics and Applications*. 1st ed. 20. Edited by R. Korthauer. Berlin, Heidelberg: Springer Berlin Heidelberg. doi: 10.1007/978-3-662-53071-9.

Le Lostec, B., Galanis, N. and Millette, J. (2013) 'Simulation of an ammonia–water absorption chiller', *Renewable Energy*, 60, pp. 269–283. doi: 10.1016/j.renene.2013.05.027.

Macchi, E. and Astolfi, M. (2017) *Organic rankine cycle (ORC) power systems : technologies and applications*. Amsterdam, Netherlands: Woodhead Publishing.

Mago, P. J. and Hueffed, A. K. (2010) 'Evaluation of a turbine driven CCHP system for large office buildings under different operating strategies', *Energy and Buildings*, 42(10), pp. 1628–1636. doi: https://doi-org.libproxy.tuni.fi/10.1016/j.enbuild.2010.04.005.

Ministry of Environment (2007) 'D1: Water and Waste Water Systems: Regulations and Guidelines 2007. The National Building Code of Finland.', *Finnish*, p. 64.

Mission Innovation (2020) 'Sand-Based High Temperature Seasonal Heat Storage by Polar Night Energy Oy Avoided Emissions Framework-Level 2 version 0.8 assessment ≈100 $MtCO_2e$/year in 2030'. Available at: www.misolutionframework.net (Accessed: 23 May 2022).

Mohsenipour, M. *et al.* (2020) 'Design and evaluation of a solar-based trigeneration system for a nearly zero energy greenhouse in arid region', *Journal of Cleaner Production*, 254, p. 119990. doi: https://doi-org.libproxy.tuni.fi/10.1016/j.jclepro.2020.119990.

Al Moussawi, H., Fardoun, F. and Louahlia-Gualous, H. (2016) 'Review of tri-generation technologies: Design evaluation, optimization, decision-making, and selection approach', *Energy Conversion and Management*, 120, pp. 157–196. doi: https://doi-org.libproxy.tuni.fi/10.1016/j.enconman.2016.04.085.

Myllymaa, T., Holmberg, H. and Ahtila, P. (2019) 'Techno-economic evaluation of biomass drying in moving beds: The effect of drying kinetics on drying costs', *Drying technology*, 37(10), pp. 1201–1214. doi: 10.1080/07373937.2018.1492615.

Pethurajan, V., Sivan, S. and Joy, G. C. (2018) 'Issues, comparisons, turbine selections and applications – An overview in organic Rankine cycle', *Energy conversion and management*, 166, pp. 474–488. doi: 10.1016/j.enconman.2018.04.058.

Quoilin, S. *et al.* (2013) 'Techno-economic survey of Organic Rankine Cycle (ORC) systems', *Renewable & sustainable energy reviews*, 22, pp. 168–186. doi: 10.1016/j.rser.2013.01.028.

REMER, D. S. and CHAI, L. H. (1990) 'Design cost factors for scaling-up engineering equipment', *Chemical engineering progress*, 86(8), pp. 77–82.

Richard K Ellsworth (2009) 'CAPACITY FACTOR COST MODELING FOR GAS-FIRED POWER PLANTS', *Construction Accounting & Taxation*, 19(1), p. 30.

Ritchie, H., Roser, M. and Rosado, P. (2020) *Energy Production and Consumption*.

Available at: https://ourworldindata.org/energy-production-consumption#citation (Accessed: 30 March 2022).

Sarkar, J., Bhattacharyya, S. and Gopal, M. R. (2006) 'Simulation of a transcritical CO2 heat pump cycle for simultaneous cooling and heating applications', *International Journal of Refrigeration*, 29(5), pp. 735–743. doi: 10.1016/J.IJREFRIG.2005.12.006.

Serth, R. W. (2007) *Process heat transfer principles and applications*. Amsterdam ; Elsevier Academic Press.

Shi, Y., Liu, M. and Fang, F. (2017) *Combined Cooling, Heating, and Power Systems : Modeling, Optimization, and Operation*. Newark: John Wiley & Sons, Incorporated. Available at: http://ebookcentral.proquest.com/lib/tampere/detail.action?docID=4883049.

Solar Off-Grid Lithium Battery Banks | BigBattery (no date). Available at: https://bigbattery.com/solar/ (Accessed: 24 May 2022).

Tocci, L. *et al.* (2017) 'Small Scale Organic Rankine Cycle (ORC): A Techno-Economic Review', *Energies (Basel)*, 10(4), p. 413. doi: 10.3390/en10040413.

Tyagi, H. *et al.* (2018) *Applications of Solar Energy*. 1st edn. Singapore: Springer Singapore. doi: 10.1007/978-981-10-7206-2.

Tyrjy, T. T., Aquarius, H. and Hiittenharju, J. (no date) *Energiakatselmuksesta käytäntöön Hotellien energiankulutus hallintaan*. Available at: www.comma.fi (Accessed: 9 March 2022).

VDI Heat Atlas. 2nd ed. 2010. (2010). Berlin, Heidelberg: Springer Berlin Heidelberg (VDI-Buch). doi: 10.1007/978-3-540-77877-6.

Wang, D. *et al.* (2013) 'Efficiency and optimal performance evaluation of organic Rankine cycle for low grade waste heat power generation', *Energy (Oxford)*, 50, pp. 343–352. doi: 10.1016/j.energy.2012.11.010.

Welcome to CoolProp — CoolProp 6.4.1 documentation (no date). Available at: http://www.coolprop.org/index.html#what-is-coolprop (Accessed: 28 March 2022).

Zhang, X. *et al.* (2021) 'Arbitrage analysis for different energy storage technologies and strategies', *Energy Reports*, 7, pp. 8198–8206. doi: 10.1016/J.EGYR.2021.09.009.

Ziher, D. and Poredos, A. (2006) 'Economics of a trigeneration system in a hospital', *Applied Thermal Engineering*, 26(7), pp. 680–687. doi: https://doi-org.libproxy.tuni.fi/10.1016/j.applthermaleng.2005.09.007.